Published for SISSA by Springer

Received: *October 22, 2024*
Revised: *January 7, 2025*
Accepted: *February 3, 2025*
Published: *February 27, 2025*

Search for high-mass resonances in a final state comprising a gluon and two hadronically decaying W bosons in proton-proton collisions at $\sqrt{s} = 13$ TeV

The CMS collaboration

E-mail: cms-publication-committee-chair@cern.ch

Abstract: A search for high-mass resonances decaying into a gluon, g, and two W bosons is presented. A Kaluza-Klein gluon, g_{KK}, decaying in cascade via a scalar radion R, $g_{KK} \to gR \to gWW$, is considered. The final state studied consists of three large-radius jets, two of which contain the products of hadronically decaying W bosons, and the third one the hadronization products of the gluon. The analysis is performed using proton-proton collision data at $\sqrt{s} = 13$ TeV collected by the CMS experiment at the CERN LHC during 2016–2018, corresponding to an integrated luminosity of 138 fb^{-1}. The masses of the g_{KK} and R candidates are reconstructed as trijet and dijet masses, respectively.These are used for event categorization and signal extraction. No excess of data events above the standard model background expectation is observed. Upper limits are set on the product of the g_{KK} production cross section and its branching fraction via a radion R to gWW. This is the first analysis examining the resonant WW+jet signature and setting limits on the two resonance masses in an extended warped extra-dimensional model.

Keywords: Beyond Standard Model, Hadron-Hadron Scattering, Jets, Vector Boson Production

ArXiv ePrint: 2410.17303

https://doi.org/10.1007/JHEP02(2025)199

JHEP02(2025)199

Contents

1 Introduction

The search for extensions of the standard model (SM) remains one of the most important goals of the CERN LHC research program. Beyond-the-SM (BSM) physics can manifest itself through the production of a new heavy particle that decays into SM particles. Numerous searches for massive resonances decaying into a pair of SM particles, such as dijet or diboson searches [1–15], have been conducted without resulting in any compelling evidence for BSM physics.

Several BSM theories can also give rise to resonances resulting in signatures with three or more SM bosons. Extended models with warped extra dimensions [16–21] are among those that predict such a signal. These models assume a Randall-Sundrum scenario with an extended bulk space containing two branes in addition to the one on which the SM resides [16]. Each additional brane introduces a bulk scalar boson, the radion R, which stabilizes the size of the extra dimension through the potential of a modulus field [22]. One of the main motivations of these models is to tackle the SM hierarchy problem [23, 24], where quantum corrections to the Higgs boson mass need to be fine-tuned to the ratio $(M_{\mathrm{EW}}/M_{\mathrm{Pl}})^2$ in order to maintain the Higgs boson mass at the observed electroweak scale, with M_{EW} and M_{Pl} representing the electroweak and Planck scales, respectively. Extended warped extra-dimensional models address the M_{Pl}–M_{EW} gap by proposing that it is an artifact of the SM not residing in the full bulk space, while simultaneously addressing flavor hierarchy problems. Such BSM signatures would, however, remain undetected in the above-mentioned dijet and diboson resonance searches since their final states are not fully reconstructed. Therefore, dedicated searches are needed.

Previous searches for triboson and trigluon signatures resulting from a two-step cascade decay of a heavy resonance have been performed by the CMS experiment [25–28]. A scenario containing a W boson plus two gluons (g) has been probed by the ATLAS experiment [29]. Despite the constraints imposed by these searches, a large fraction of the theoretical parameter space remains unexplored. In this paper, we consider the specific extended warped extra-dimensional scenario in which only the quantum chromodynamic (QCD) gauge field can propagate into the extended bulk, giving rise to a Kaluza-Klein (KK) gluon $\mathrm{g_{KK}}$. The $\mathrm{g_{KK}}$ can decay in a cascade through the lightest radion of the theory. In a certain parameter space of the model, the dominant decay mode is $\mathrm{g_{KK}} \to \mathrm{gR} \to \mathrm{gWW}$, which has not yet been directly probed, and is the focus of this analysis.

In this paper, we probe the gWW signature performing a search for BSM physics in the trijet final state. Two of the jets, both arising from the posited R decay, are identified using jet substructure techniques as originating from hadronic decays of Lorentz-boosted W bosons. No particular requirements are imposed on the third jet, which, in this model, is expected to originate from the gluon. This choice preserves search generality as it allows other potential signals to be selected. Figure 1 displays a schematic diagram of the signal process, including the cascade decay and the resulting final state probed in this paper. The overall $\mathrm{g_{KK}}$ mass range explored is 1.25–4.5 TeV. Within this range, the phase space with a ratio of R and $\mathrm{g_{KK}}$ masses of $0.04 < m_{\mathrm{R}}/m_{\mathrm{g_{KK}}} < 0.9$ is considered. For $m_{\mathrm{R}}/m_{\mathrm{g_{KK}}} < 0.2$ and $m_{\mathrm{R}}/m_{\mathrm{g_{KK}}} > 0.8$, the analysis sensitivity is reduced because a significant number of events result in a dijet final state that is not selected. In the former case, the two W bosons are collimated, while in the latter case, the final-state gluon carries relatively little energy.

The analysis is based on proton-proton (pp) collision data collected by the CMS experiment during 2016–2018 at $\sqrt{s} = 13\,\mathrm{TeV}$, with integrated luminosities of 36.3 [30], 41.5 [31], and 59.7 [32] $\mathrm{fb^{-1}}$ for 2016, 2017, and 2018, respectively, yielding a total of $138\,\mathrm{fb^{-1}}$. The targeted signal is reconstructed by identifying the two W boson jet candidates, whose combined invariant mass m_{jj} yields the posited m_{R}. These jets, along with a third one, are used to reconstruct the $\mathrm{g_{KK}}$ resonance candidate and compute its invariant trijet mass m_{jjj}. To increase analysis sensitivity, m_{jj} and m_{jjj} are corrected, improving their resolution. Machine-learning techniques are employed to reconstruct and identify the jets originating from a W boson decay. In previous analyses [25, 26], the DeepAK8 algorithm [33] has been used for this purpose. In this paper, we use the ParticleNet (PNet) algorithm [34], which yields a significantly better signal selection efficiency for the same background rejection and exhibits a reduced dependency on the jet mass. Additionally, we split the selected event sample based on the ratio $m_{\mathrm{jj}}/m_{\mathrm{jjj}}$.

JHEP02(2025)199

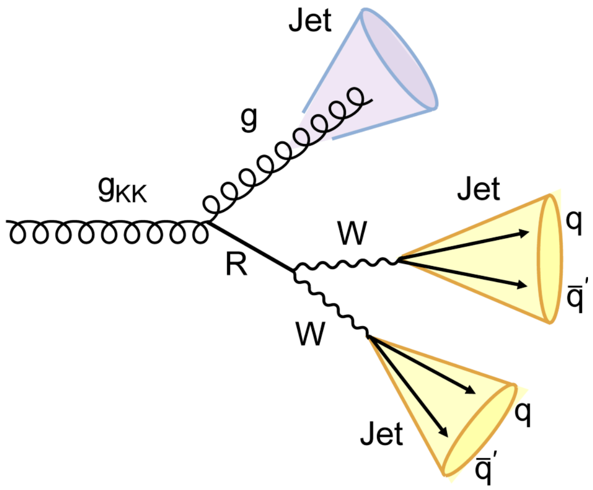

Figure 1. A schematic diagram of the decay of a g_{KK} boson via a radion R to the final state considered in this analysis.

While this search is optimized for a gWW signal, it is also sensitive to other signals containing a pair of Lorentz-boosted W or Z bosons. In particular, this includes any heavy resonance decaying, with or without an intermediate particle, into XWW, XWZ, or XZZ, where X is a particle resulting in an energetic jet, such as a light or heavy quark, a vector boson, or a BSM particle.

This paper is organized as follows: section 2 provides a description of the CMS detector. Section 3 describes the simulated samples used in the analysis. The triggers employed for data collection and the event reconstruction are discussed in section 4. The event selection and categorization are presented in section 5. Section 6 describes the estimation of the SM background. Systematic uncertainties are discussed in section 7. The results and their interpretation are given in section 8. The paper is summarized in section 9. Tabulated results for this analysis are provided in the HEPData record [35].

2 The CMS detector

The central feature of the CMS detector is a superconducting solenoid of 6 m internal diameter, providing a magnetic field of 3.8 T. A silicon pixel and strip tracker, a lead tungstate crystal electromagnetic calorimeter (ECAL), and a brass and scintillator hadron calorimeter (HCAL), each composed of a barrel and two endcap sections resides within the solenoid volume. Forward calorimeters extend the coverage provided by the barrel and endcap detectors up to pseudorapidities of $|\eta| = 5$. Muons are measured in gas-ionization detectors embedded in the steel flux-return yoke outside the solenoid.

The trijet events of interest are selected using a two-tiered trigger system. The first level, composed of custom hardware processors, uses information from the calorimeters and muon detectors to select events at a rate of around 100 kHz, making a decision within the fixed period of about 4 μs following the beam crossing, allowed by the latency implemented in the readout path [36]. The second level, known as the high-level trigger, consists of a farm of processors running a version of the full event reconstruction software optimized for fast

JHEP02(2025)199

processing, and reduces the event rate to around 1 kHz before data storage [37]. A more detailed description of the CMS detector, together with a definition of the coordinate system and kinematic variables, can be found in refs. [38, 39].

3 Simulated samples

The signal is simulated at leading order (LO) using the MadGraph5_aMC@NLO 2.4.2 generator [40], covering a wide range of g_{KK} and R masses ($m_{g_{KK}}$ from 1.25 to 4.5 TeV and m_R from 4 up to 90% of $m_{g_{KK}}$). The corresponding KK gauge coupling values that are used for the interpretation of this result are $g_{\gamma_{KK}} = 2.65$, $g_{W_{KK}} = 3$, $g_{g_{KK}} = 6$, and $g_{grav} = 5$, as proposed in ref. [17]. The widths of both g_{KK} and R are less than 2% of their masses, thus satisfying the narrow-width approximation.

The dominant SM background originates from jets produced through the strong interaction. Such events are referred to as QCD multijet events. While this background is estimated using data, the procedure is tested using simulation. The QCD multijet events, along with the subdominant background from W+jets and the Z+jets production, designated as "V+jets", are simulated at LO with MadGraph5_aMC@NLO, and matched to parton showers with the MLM [41] algorithm. The top quark-antiquark pair ($t\bar{t}$) and single top quark (t) background production are modeled at next-to-LO (NLO) in QCD using the powheg 2.0 generator [42–47]. The minor diboson background is simulated at NLO with either powheg (WW production) or MadGraph5_aMC@NLO (WZ, ZZ), collectively referred to as "VV". Contributions from other processes are found to be negligible.

The signal and background samples for all three years of data taking are generated with the LO or next-to-NLO NNPDF3.1 parton distribution functions (PDFs) [48], ensuring that the order of the PDFs matches that of the matrix element calculations. The parton showering, fragmentation, and hadronization for all samples is performed using pythia 8.230 [49] with the underlying event tune CP5 [50]. The CMS detector response is modeled using the Geant4 package [51]. The simulated events include the contribution of particles from additional pp interactions within the same or neighboring bunch crossings, referred to as pileup (PU), and are corrected to reproduce the distribution of the number of PU interactions observed in the data.

4 Event reconstruction

The primary interaction vertex (PV) is taken to be the vertex corresponding to the hardest scattering in the event, evaluated using tracking information alone, as described in section 9.4.1 of ref. [52].

The particle-flow (PF) algorithm [53] aims to reconstruct and identify each interacting particle in an event, with an optimized combination of information from the various elements of the CMS detector. The energy of electrons is determined from a combination of the track momentum at the PV, the corresponding ECAL cluster energy, and the energy sum of all bremsstrahlung photons attached to the track. The energy of muons is obtained from the curvature of the corresponding track. The energy of charged hadrons is determined from a combination of their momentum measured in the tracker and the matching ECAL and

JHEP02(2025)199

HCAL energy deposits, corrected for the response function of the calorimeters to hadronic showers. Finally, the energy of neutral hadrons is obtained from the corresponding corrected ECAL and HCAL energies.

For each event, hadronic jets are clustered from these reconstructed particles using the infrared- and collinear-safe anti-k_{T} jet finding algorithm [54, 55] as implemented in the FastJet package [55]. The clustering algorithm is run twice over the same inputs with the distance parameters 0.4 and 0.8, resulting in AK4 and AK8 jet collections, respectively. Jet momentum is determined as the vectorial sum of all particle momenta in the jet, and is found from simulation to be, on average, within 5 to 10% of the true momentum over the entire transverse momentum spectrum and detector acceptance [56].

The PU per particle identification algorithm [57, 58] is used to mitigate the effect of PU in AK8 jets at the reconstructed-particle level, making use of local shape information, event PU properties, and tracking information. A local shape variable is defined, which distinguishes between collinear and soft diffuse distributions of other particles surrounding the particle under consideration. The former is attributed to particles originating from the hard scattering and the latter to particles originating from PU interactions. Charged particles identified to be originating from PU vertices are discarded. For each neutral particle, the local shape variable is computed using the surrounding charged particles compatible with the PV within the tracker acceptance ($|\eta| < 2.5$), and using both charged and neutral particles in the region outside of the tracker coverage. The momenta of the neutral particles are then rescaled according to their probability to originate from the PV deduced from the local shape variable, thus superseding the need for jet-based PU corrections [57].

Jet energy corrections are derived from simulation to bring the measured response of jets to that of particle-level jets on average. In situ measurements of the momentum balance in dijet, photon+jet, Z+jet, and multijet events are used to account for any residual differences in the jet energy scale (JES) between data and simulation [56]. The jet energy resolution (JER) measured using a dijet balance technique amounts typically to 15–20% at 30 GeV, 10% at 100 GeV, and 5% at 1 TeV [56]. Additional selection criteria are applied to each jet to remove jets potentially dominated by anomalous contributions from various subdetector components or reconstruction failures [59].

The AK4 jets originating from the hadronization of bottom (b) quarks are identified ("b tagged") using a deep neural network algorithm DeepJet [60, 61] that takes as input: tracks within the jet that are displaced from the PV, identified secondary vertices, jet kinematic variables, neutral PF candidates, and information related to the presence of soft leptons in the jet. A threshold on the DeepJet score is used, corresponding to a 0.1% probability of misidentifying a light-flavor quark or a gluon (udsg) AK4 jet with $p_{\mathrm{T}} > 30\,\mathrm{GeV}$ and $|\eta| < 2.5$ as a b quark jet, while maintaining a 67% signal efficiency.

The missing transverse momentum vector, $\vec{p}_{\mathrm{T}}^{\,\mathrm{miss}}$, is computed as the negative vector sum of the transverse momenta ($\vec{p}_{\mathrm{T}}$) of all the PF candidates in an event, and its magnitude is denoted as $p_{\mathrm{T}}^{\mathrm{miss}}$ [62]. The $\vec{p}_{\mathrm{T}}^{\,\mathrm{miss}}$ is modified to account for corrections to the energy scale of the reconstructed jets in the event. Anomalous high-$p_{\mathrm{T}}^{\mathrm{miss}}$ events can occur due to a variety of reconstruction failures, detector malfunctions, or noncollision backgrounds. Such events are rejected by conditions that are designed to identify more than 85–90% of the spurious high-$p_{\mathrm{T}}^{\mathrm{miss}}$ events with a single efficiency loss of less than 0.1% [62].

JHEP02(2025)199

The AK8 jets containing hadronic decays of W bosons are identified using the PNet machine learning algorithm [34], with PF candidates and secondary vertices as input. The algorithm output classifies jets by assigning one score for each class trained. The algorithm is used in its mass-decorrelated version [63]. For the identification of W bosons, the ratio of the PNet scores of the $\mathrm{W} \to \mathrm{q\overline{q}'}$ class to the sum of all QCD multijet classes is formed and referred to as $\mathrm{PNet_W}$ in the following. We additionally make use of the groomed jet mass (m_j) for further discrimination of W boson jets from background jets. The groomed jet mass is calculated after applying a modified mass-drop algorithm [64, 65] to AK8 jets, with parameters $\beta = 0$, $z_\mathrm{cut} = 0.1$, and $R_0 = 0.8$ also known as the *soft drop* algorithm [66]. The variables are calibrated in a $\mathrm{t\overline{t}}$ enriched sample with hadronically decaying W boson [67]. Further details on the calibration method used for this analysis are given in section 6. The soft-drop mass is meant when referring to the jet mass in the following.

Isolated muon and electron candidates, collectively referred to as leptons ℓ in the following, are reconstructed as follows in order to veto events containing them. Muon candidates are required to fulfill $p_\mathrm{T} > 20\,\mathrm{GeV}$, to be within the geometrical acceptance of the muon detectors ($|\eta| < 2.4$), and are reconstructed by combining the information from the silicon tracker and the muon chambers [68]. Electron candidates with $p_\mathrm{T} > 35\,\mathrm{GeV}$ and within $|\eta| < 2.5$ are reconstructed using an algorithm that associates fitted tracks in the silicon tracker with electromagnetic energy clusters in the ECAL [69]. Electron candidates identified as coming from photon conversions in the detector are also rejected. Identified muons and electrons are required to be isolated from hadronic activity in the event. The isolation variable is defined by summing the p_T of all the PF candidates in a cone of radius $\Delta R = \sqrt{(\Delta\eta)^2 + (\Delta\phi)^2} = 0.4\,(0.3)$ around the muon (electron) track, where ϕ is the azimuthal angle in radians, and is corrected for the contribution of neutral particles from PU interactions [68, 69].

5 Event selection

5.1 Trigger

Several triggers are used to select events of interest. One set of triggers requires H_T, the scalar sum of the p_T of all AK4 jets (with $p_\mathrm{T} > 30\,\mathrm{GeV}$ and $|\eta| < 2.4$) in the event, to be greater than 800, 900, or 1050 GeV, depending on the data-taking era. In addition, single high-p_T jet triggers are used for the 2016 era. Furthermore, events containing a high-p_T AK8 jet with trimmed mass [70] in combination with either H_T calculated using AK8 jets or single AK8 jet p_T requirements are selected. The choice of triggers is identical to the one used in a similar analysis described in ref. [26], where more details can be found. The combination of all triggers (logical OR) results in a selection efficiency greater than 99% over the full data set, for events with $H_\mathrm{T} > 1.1\,\mathrm{TeV}$, as measured using AK8 jets in an independent sample of data events collected with a single-muon trigger and found to be consistent for both data and simulated samples.

5.2 Preselection and signal region

Two stages of event selection are implemented. The first, the preselection, is initially applied to select events with signal-like kinematic features, comparing them to the SM backgrounds.

JHEP02(2025)199

A more stringent selection, the signal region (SR) selection, is then applied to further improve the background rejection and define the event sample used in the statistical analysis. The AK8 jets will simply be referred to as "jets" in the following.

The preselection requires exactly three jets, corresponding to the two W boson candidates and the gluon candidate, for consistency all reconstructed as AK8 jets, with $p_{\mathrm{T}}^{\mathrm{j}} > 200\,\mathrm{GeV}$, $|\eta_{\mathrm{j}}| < 2.4$, and with the highest p_{T} jet satisfying also the $p_{\mathrm{T}}^{\mathrm{j1}} > 400\,\mathrm{GeV}$ condition. The event H_{T} is required to exceed 1.1 TeV to ensure that the fully efficient trigger. The jets with the highest and second-highest $\mathrm{PNet_W}$ score, designated as ja and jb, respectively, are taken as the two W boson candidates of the event while the third one, jc, is assumed to be the gluon. The probability of incorrectly assigning at least one jet in this way is approximately 20% at the preselection level, and, e.g., 7% in the SR for $m_{\mathrm{g_{KK}}} = 2\,\mathrm{TeV}$ and $m_{\mathrm{R}} = 1\,\mathrm{TeV}$. The masses of ja and jb, m_{ja} and m_{jb}, must each be greater than 50 GeV, while no requirement is imposed on the jc mass, m_{jc}. Events containing isolated leptons are rejected.

The ja (jb) $\mathrm{PNet_W}$ score, designated as s_{ja} (s_{jb}), is required to be greater than 0.9 (0.8). These conditions correspond to selection efficiencies of approximately 33 (43)% and 0.5 (1.3)% for signal and background jets, respectively (evaluated over a generic sample of jets other than from the analysis preselection). The s_{ja} and s_{jb} spectra for signal and background events at the preselection are presented in figure 2, upper left and right, respectively. The combined s_{ja} and s_{jb} conditions at the preselection yield a 36–45% signal efficiency (varying with jet p_{T}) and 2% (3%) background efficiency in simulation (data). Based on the s_{jb} value, events are divided into two categories, SRa and SRb, with the requirements $s_{\mathrm{jb}} > 0.9$ and $0.8 < s_{\mathrm{jb}} < 0.9$, respectively. This binning enhances the analysis sensitivity by defining SRa with high signal purity and low background, complemented by SRb with moderate purity and higher background.

We define the observable m_{85} as $m_{85} \equiv \sqrt{(m_{\mathrm{ja}} - 85\,\mathrm{GeV})^2 + (m_{\mathrm{jb}} - 85\,\mathrm{GeV})^2}$. The value of 85 GeV is chosen since the reconstructed signal W boson mass peaks near that value, as shown in figure 3 (upper left), due to additional radiation captured within the jet cone.

We require the W boson jet candidates to be compatible with that mass by requiring $m_{85} < 15\,\mathrm{GeV}$. Figure 3 presents the m_{ja} and m_{jb} distributions (upper left) and the m_{85} variable (upper right) after the preselection. The first and the last bins of the one-dimensional distributions of figure 3 contain the events outside the illustrated range.

The QCD multijet background is further reduced by requiring that the largest absolute difference in pseudorapidity found among the three possible jet pairs is $|\Delta\eta_{\mathrm{jj}}^{\mathrm{max}}| < 3$. Events arising from $\mathrm{t\bar{t}}$ and single t quark production result in final states with b-tagged jets. To suppress this background, events that contain b-tagged AK4 jets are rejected using the DeepJet algorithm, as described in section 4.

5.3 Resonance reconstruction and event categorization

The masses of the R and $\mathrm{g_{KK}}$ resonance candidates can be reconstructed using the invariant masses of the two W boson candidate jet system $m_{\mathrm{jajb}} \equiv m_{\mathrm{jj}}$, and of all three jets $m_{\mathrm{jajbjc}} \equiv m_{\mathrm{jjj}}$, respectively. In approximately 94% of all cases, the W bosons resulting from the decay of the R boson are correctly identified by the PNet algorithm. For most of the remaining cases, the W boson decay products are not contained in a single AK8 jet.

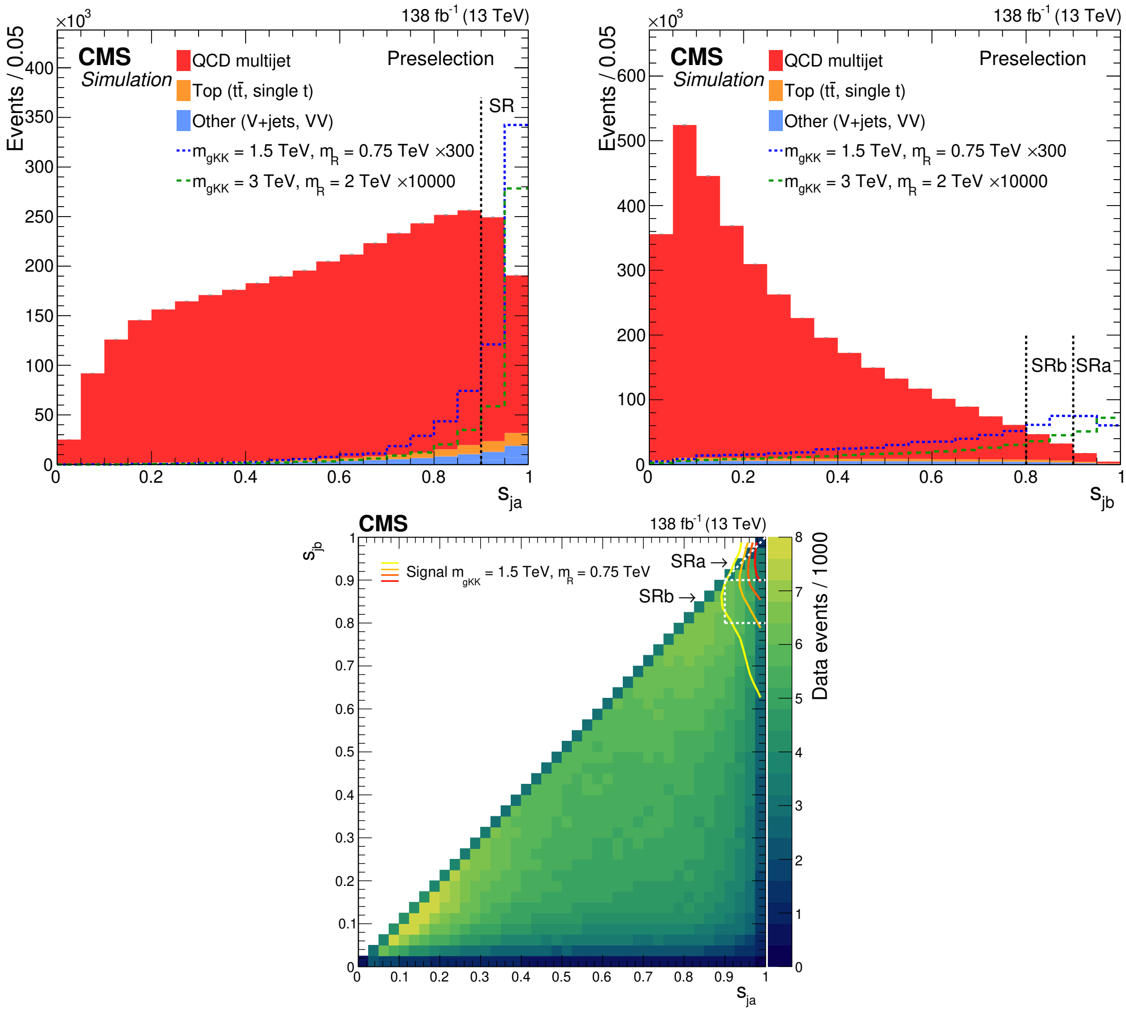

Figure 2. Upper left (right): the one-dimensional distributions of s_{ja} (s_{jb}) for the labeled signal scenario compared to the simulated background. Black dashed lines indicate the SR selection boundaries. Lower: the two-dimensional (s_{ja}, s_{jb}) distribution in data. For the hypothesized signal ($m_{\mathrm{R}} = 0.75\,\mathrm{TeV}$, $m_{\mathrm{g_{KK}}} = 1.5\,\mathrm{TeV}$), contours representing constant event yield fractions (80, 60, 40, and 20% of the maximum yield) are shown to illustrate the shape. White dashed lines indicate the boundaries between SRa, SRb samples, and regions of rejected events. All distributions are shown after event preselection.

Instead of using these two masses directly, we are using modified versions, in which the jet masses are subtracted, and the average expected W boson mass estimated from simulation is added. This strategy leads to an improved signal resolution due to the detector resolution effects canceling out. These variables are defined and designated as $m^*_{\mathrm{jj}} \equiv m_{\mathrm{jj}} - m_{\mathrm{ja}} - m_{\mathrm{jb}} + 2 \times 85\,\mathrm{GeV}$, and $m^*_{\mathrm{jjj}} \equiv m_{\mathrm{jjj}} - m_{\mathrm{ja}} - m_{\mathrm{jb}} + 2 \times 85\,\mathrm{GeV}$. An improvement in sensitivity of 10 (4)% for m^*_{jj} (m^*_{jjj}) is observed. Figure 3 (middle row) presents the corrected distributions of m^*_{jj} (left) and m^*_{jjj} (right) in simulation after preselection.

Events are divided into five orthogonal regions based on the ratio $m^*_{\mathrm{jj}}/m^*_{\mathrm{jjj}}$ to better probe different R masses. The corresponding SRs are enumerated (from lower to higher ratio values) as SR1–SR5. The SR1–5 ranges over $m^*_{\mathrm{jj}}/m^*_{\mathrm{jjj}}$ are symmetrically located around 0.5,

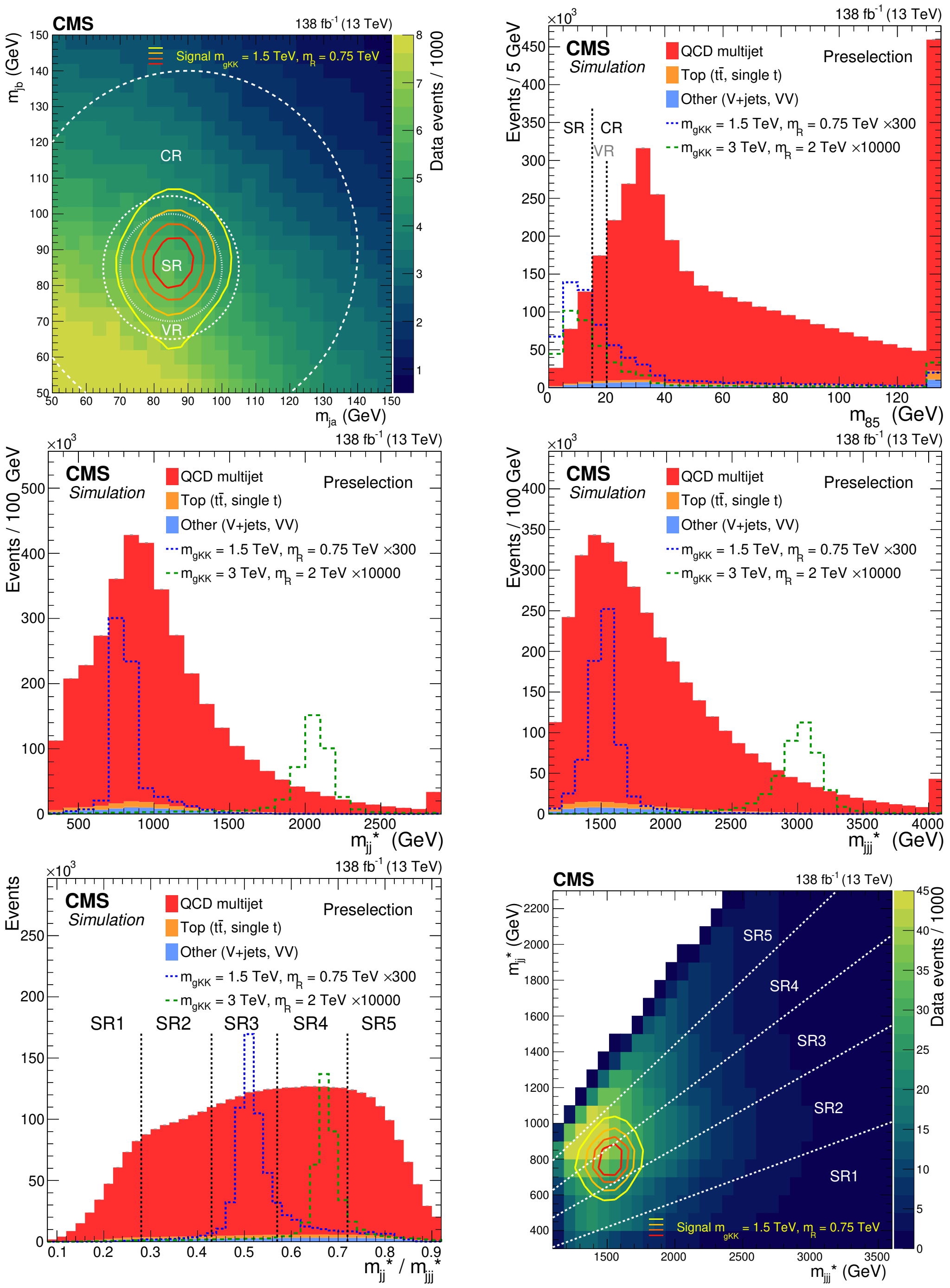

Figure 3. Distributions after event preselection. Upper left: the two-dimensional (m_{ja}, m_{jb}) distribution for a posited signal ($m_{\mathrm{R}} = 0.75$ TeV, $m_{\mathrm{g_{KK}}} = 1.5$ TeV) compared to the background-dominated data. For signal, contours corresponding to 80, 60, 40, and 20% of the maximum signal event yield are shown for shape visualization. White dashed curves indicate boundaries between SR, VR (defined in section 6.1), and CR areas. The one-dimensional histograms show the m_{85} (upper right), m^*_{jj} (middle left), m^*_{jjj} (middle right), and $m^*_{\mathrm{jj}}/m^*_{\mathrm{jjj}}$ (lower left) distributions using simulated signal and background events, as indicated in the legends. The signal events are scaled by the labeled factors times the theoretical cross sections for visibility. Lower right: the two-dimensional (m^*_{jj}, m^*_{jjj}) distribution in data. White dashed lines indicate the SR splitting.

JHEP02(2025)199

Region	$m^*_{\mathrm{jj}}/m^*_{\mathrm{jjj}}$	s_{jb}
SR1a	<0.28	>0.9
SR1b		0.8–0.9
SR2a	0.28–0.43	>0.9
SR2b		0.8–0.9
SR3a	0.43–0.57	>0.9
SR3b		0.8–0.9
SR4a	0.57–0.72	>0.9
SR4b		0.8–0.9
SR5a	>0.72	>0.9
SR5b		0.8–0.9

Table 1. Definition of the different SRs based on the $m^*_{\mathrm{jj}}/m^*_{\mathrm{jjj}}$ ratio and s_{jb}.

with the widths exceeding the signal resolution and dividing the data into sub-samples with approximately similar event counts, while ensuring sufficient numbers of events for QCD background predictions, as discussed in section 6.1. This categorization, together with the one based on the tagger score s_{jb}, results in a total of ten SRs designated as SR1a, SR1b, ..., SR5b. The conditions defining these SRs are summarized in table 1. The optimization of selection conditions, aiming to maximize the signal significance (defined as the ratio of the number of signal events to the square root of the number of background events), is evaluated for several signal scenarios at both the preselection level and in the SR, excluding one variable condition at a time.

The $m^*_{\mathrm{jj}}/m^*_{\mathrm{jjj}}$ distribution with the SRs indicated is shown in figure 3 (lower left). The two-dimensional distribution of m^*_{jj} vs. m^*_{jjj} is presented in the same figure (lower right). A posited signal is illustrated with constant yield contours and is centered around the generated m_{R} and $m_{\mathrm{g_{KK}}}$ values. The m^*_{jjj} variable is used for the statistical analysis of the data and the signal extraction in these ten SRs.

6 Background estimation

The SM backgrounds in the SRs are grouped into three categories: "QCD multijet", "Top", and "Other". The dominant background in all SRs stems from QCD multijet events, amounting to 55–75% of the total yield based on simulation, depending on the SR. Single and pair production of top quarks, collectively referred to as "Top", accounts for 7–17% of total events. All other background processes are designated as "Other". They make up 20–40% of the total events, the largest contribution coming from W+jets production.

6.1 Estimation of the QCD multijet background

The PNet tagger drastically suppresses the dominant background due to QCD multijet production leaving only relatively few simulated events in the SRs. These are difficult to predict reliably using simulation. Thus, we estimate this background contribution directly from control regions (CRs) in data. Ten CRs are used for this purpose, each in association with a corresponding SR, i.e., CR1a–CR5b. The selection defining the CRs is identical to that in the corresponding SRs as listed in table 1, except that the m_{85} requirement is inverted such that $m_{85} > 15\,\mathrm{GeV}$. In addition, a new variable defined as $m_{90} = \sqrt{(m_{\mathrm{ja}} - 90\,\mathrm{GeV})^2 + (m_{\mathrm{jb}} - 90\,\mathrm{GeV})^2}$ is introduced, imposing $m_{90} < 50\,\mathrm{GeV}$. In the $(m_{\mathrm{ja}},\, m_{\mathrm{jb}})$ plane shown in figure 3 (upper left) SR and CR are indicated. In this illustration, the area with $15 < m_{85} < 20\,\mathrm{GeV}$, while also part of the CR, is used as a validation region (VR). The distribution of events in the $(m_{\mathrm{ja}},\, m_{\mathrm{jb}})$ plane is not homogeneous. By using nonconcentric circles (m_{85} in SRs vs. m_{90} in CRs), we ensure that the average jet masses (m_{ja} and m_{jb}) remain approximately the same in both the SR and CR. Since m^*_{jjj} depends on m_{ja} and m_{jb}, defining CRs using m_{90} ensures kinematic consistency between the CR and SR, avoiding potential biases in the m^*_{jjj} prediction. The m^*_{jjj} spectra in simulated QCD multijet samples are found to be consistent between SRs and CRs within their statistical uncertainties.

Based on simulation, about 90% of the events in the CRs are QCD multijet events. Their kinematic properties are very similar to those of the QCD multijet events in the SRs. Most importantly, CR events feature the same selection efficiency as the SR events, as the $\mathrm{PNet_W}$ tagger condition remains identical.

The m^*_{jjj} spectra of QCD multijet events in SRs are predicted using the data in the CRs. All other SM processes labeled as "Rest" in the following are subtracted using simulation. Each resulting CR template is scaled to the event yields of the corresponding SR using the ratio of total simulated QCD multijet events in the given SR and CR, $\mathrm{QCD_{SRxy}}/\mathrm{QCD_{CRxy}}$. This can be written as:

$$\mathrm{Pred}^{\mathrm{QCD}}_{\mathrm{SRxy}} \equiv [\mathrm{Data} - \mathrm{Rest}]_{\mathrm{CRxy}} \frac{\mathrm{QCD_{SRxy}}}{\mathrm{QCD_{CRxy}}}. \tag{6.1}$$

The QCD multijet event yields obtained in this way are factors of 1.6–1.8 larger than predicted by the simulation depending on the SR. These differences are consistent with similar analyses [25, 26], reflecting the limitations of QCD multijet modeling at high tagger scores.

6.2 Estimation of the Top and Other backgrounds

The normalization and the shape of the Top background is estimated from simulation and validated in data CRs. For this purpose, we are using the data from ten regions, defined similarly to the SRs, but requiring the presence of at least one b-tagged AK4 jet. These b-tagged jet enriched regions are called bRs in the following. The signal contribution in the bRs is an order of magnitude lower than in the SRs, and thus negligible. According to simulation, the bRs consist to approximately 70, 25, and 5% of Top, QCD multijet, and Other processes, respectively. The QCD multijet contribution in each bR_{xy} is estimated using simulation, corrected by the factor $[\mathrm{Data} - \mathrm{Rest}]_{\mathrm{CRxy}}/\mathrm{QCD_{CRxy}}$ obtained from the corresponding CRxy. The remaining difference with respect to the data in each bR, ranging

JHEP02(2025)199

Jet p_T (GeV)	200–300	300–400	>400
$s_{ja} > 0.9$	0.83 ± 0.03	0.84 ± 0.04	0.82 ± 0.05
$0.8 < s_{jb} < 0.9$	1.08 ± 0.03	1.01 ± 0.04	1.02 ± 0.05

Table 2. The $\mathrm{PNet_W}$ scale factors calculated for exclusive p_T and $\mathrm{PNet_W}$ tagger score ranges of W boson matched jets.

from 0 to 50%, is then attributed to the Top background. A 50% rate uncertainty in the Top production cross section, uncorrelated across the SRs, is assigned. The Top background m^*_{jjj} shapes in the bRs are found to be consistent with simulation within uncertainties.

The contribution of the Other background in the SRs is estimated from simulation. It is dominated by W+jets production, which accounts for approximately two thirds of the events. The selections used in this analysis, in particular the vetoing of leptons and selecting two W boson candidates, do not allow the definition of a pure W+jets sample close to the SR. However, a similar triboson analysis [25], for which W+jets production was the dominant background, found this process to be well-described by simulation. A conservative 30% uncertainty is assigned to the Other background rate. A correction is applied to both Top and Other background simulations to account for the differences in the PNet W boson selection efficiency in data and simulation, as described below.

6.3 Calibration of the W boson tagger

For the QCD multijet background, an estimate using the same selection conditions on s_{ja} and s_{jb} in the data CRs and SRs, obviates the need for correcting the PNet selection efficiency. For the signal and all other background processes that contain genuine W bosons, the PNet selection efficiency is calibrated using the data. By requiring the data to match the simulation in the jet mass distribution, scale factors (SFs) are derived for the selected W boson candidate jet with $\mathrm{PNet_W}$ scores of 0.8–0.9 and >0.9. These SFs are binned in jet p_T and summarized in table 2.

To apply the SFs, all reconstructed jets in simulated events are subjected to matching with the generated partons using geometrical conditions, as described in ref. [26]. Both the simulated signal and background events are corrected with these SFs for each jet matched as a W boson, across all samples used in the analysis and in all regions.

6.4 Background estimation validation

The background estimation method is validated in the data without using the actual SR events. Instead, SRs are replaced by ten VRs. These are obtained using the SR selection conditions given in table 1, changing only the $m_{85} < 15\,\mathrm{GeV}$ condition to $15 < m_{85} < 20\,\mathrm{GeV}$, as illustrated in figure 3, upper row. As the $15 < m_{85} < 20\,\mathrm{GeV}$ range nominally is part of the CRs, for this test only, the CRs are redefined excluding these overlapping events. The prediction of the shape and rate of QCD multijet production is evaluated for each VR with the same method as used for the SRs. Simulation is used for processes other than QCD multijet, as their contribution is small outside the W boson mass window. A maximum likelihood fit is performed, including all the sources of systematic uncertainty described in

Uncertainty source	B or S	Effect on	Magnitude	Number of NPs & correlations
Normalization QCD multijet	B	Rate	20%	10, uncorr. across SRs
Normalization Top	B	Rate	50%	10, uncorr. across SRs
Normalization Other	B	Rate	30%	10, uncorr. across SRs
QCD multijet B shape due to m_{90} usage	B	Shape	$\pm 1\sigma$ templates	10, uncorr. across SRs
QCD multijet B shape due to other processes	B	Shape	$\pm 1\sigma$ templates	10, uncorr. across SRs
PU reweighting & integrated luminosity	S	Rate	1.7%	1, correlated across all SRs
PDFs	S	Rate	<10%	1, correlated across all SRs *
μ_R and μ_F scales	S	Rate	<0.8%	1, correlated across all SRs *
PNet$_W$ selection efficiency per jet (event)	S	Shape	6% (12%)	1, correlated across all SRs
JES	S	Shape	$\pm 1\sigma$ templates	1, correlated across all SRs *
JER	S	Shape	$\pm 1\sigma$ templates	1, correlated across all SRs *

Table 3. The sources of systematic uncertainties accounted for in the analysis. From left to right: indication of whether an uncertainty is evaluated for the background (B) or signal (S), whether the uncertainty affects shape or rate, magnitudes (where applicable, or standard deviations (σ)), and the total number of nuisance parameters (NPs) used along with their correlations across SRs. The "*" indicates a value or a shape template different for each signal scenario.

section 7 for the actual result interpretation. The observed $m^*_{\rm jjj}$ distributions in data agree with the predicted ones within statistical uncertainties, validating the prediction method described in section 6.1. The maximum nonclosure observed in the VRs prior to the fit is assigned as the uncertainty in the QCD background rate.

7 Systematic uncertainties

Systematic uncertainties are taken into account for the background estimation and the signal extraction. For each source of uncertainty, a nuisance parameter is assigned, which is constrained by the data. These are summarized in table 3. Uncertainties in the background estimation and signal modeling are grouped separately. It is also indicated whether the uncertainty is in the $m^*_{\rm jjj}$ shape or the rate of a particular process.

7.1 Systematic uncertainties in the background estimation

7.1.1 Systematic uncertainties in the background rates

The three background categories (defined as QCD multijet, Top, and Other) are assigned normalization rate uncertainties of magnitude 20, 50, and 30%, respectively, with a log-normal prior. One nuisance is used for each background category and for each SR, resulting in a total of 30 nuisance parameters. The 20% magnitude of the QCD multijet background category is obtained from the maximum nonclosure observed in the VRs before performing the fit and from the statistical uncertainty in the ratio factor of eq. (6.1), resulting from simulation. The observed modeling of the PNet$_{\rm W}$ score and the $m^*_{\rm jj}/m^*_{\rm jjj}$ distributions at the preselection level supports the choice of using uncorrelated nuisance parameters across the SRs. A 20% uncertainty is assigned to account for residual differences between the simulation and the data. The 50% magnitude of the Top category is assessed by the maximum nonclosure observed in the bRs. The 30% magnitude of the Other category, since it is dominated by the W+jets production, is assessed from a similar analysis [25] where the W+jets process is the dominant background. Uncertainties in the JES and JER of the simulated backgrounds were found to have a negligible impact on the final result.

7.1.2 Systematic uncertainties in the QCD multijet background shape

The $m^*_{\rm jjj}$ shape of the QCD multijet background is assigned two uncertainties. As the shape comes effectively from the data in the CRs, as eq. (6.1) denotes, the prediction is susceptible to potential biases due to:

(a) the choice of the circular area in the ($m_{\rm ja}$, $m_{\rm jb}$) plane used to define the CRs, which is centered around (90, 90) GeV (figure 3 upper left), i.e., the choice of using m_{90}, and

(b) the subtraction of the largely unknown rate of backgrounds other than QCD multijet production in the prediction method (given by eq. (6.1)).

For (a), we derive two alternative shape predictions ($\pm 1\sigma$ variations) using two modified CR selection conditions: $m_{85} < 50\,\text{GeV}$, and $m_{95} < 50\,\text{GeV}$, where m_{95} is defined using 95 GeV in analogy with m_{85}. In this way, we parametrize the CR definition based on the center of CR area allowing the prediction to be only loosely dependent on the nominal m_{90} used. For (b), to account for a potentially inaccurate normalization of the Other processes in CR, we derive the QCD multijet shape estimate scaling the Rest events in eq. (6.1) by factors of zero and two, also obtaining up and down variations of the $m^*_{\rm jjj}$ shape.

A nuisance parameter with a Gaussian prior is assigned for each of the two sources of uncertainty and for each of the ten SRs, resulting in 20 nuisances. These QCD multijet shape uncertainties provide flexibility in particular for the tails of the $m^*_{\rm jjj}$ spectra to adapt to a potentially softer or harder spectrum observed in the SR.

7.1.3 Systematic uncertainties in the signal rate

The simulated PU distribution is scaled to match the data using an effective total inelastic cross section of 69.2 mb. The uncertainty in this procedure is evaluated by varying the total inelastic cross section by ±4.6% [71]. This results in a 0.5% uncertainty in the signal normalization in the SRs with negligible shape effects. The uncertainty in the integrated luminosity individually for the 2016, 2017, and 2018 data-taking years amounts to 1.2–2.5% [30–32]. The overall uncertainty for the 2016–2018 period is 1.6%. The two sources are combined to a total uncertainty of 1.7%, implemented with a log-normal prior.

The renormalization $\mu_{\rm R}$ and factorization $\mu_{\rm F}$ scales, and PDF uncertainties affecting the signal selection efficiency are evaluated per SR and mass point. The scale uncertainties are obtained by varying $\mu_{\rm R}$ and $\mu_{\rm F}$ independently by factors of 1/2 and 2 (without considering the extreme cases of the opposite-direction variations). Half of the maximum difference of these variations is taken as the uncertainty with a log-normal prior, resulting in a <0.8% effect on the signal rate. The PDF uncertainties are evaluated using the replicas of the NNPDF PDF set, for each signal scenario individually. The corresponding Hessian members of the PDF set are varied, and the quadratic sum of the variations from the central value is calculated for each SR. The resulting variation in signal event yields is 0–10% for different

JHEP02(2025)199

g_{KK} masses. For the overall signal scale uncertainty, a single nuisance parameter is used to account for both the μ_R and μ_F scales, and PDF uncertainties with a log-normal prior.

7.1.4 Systematic uncertainties in the signal shape

The JES uncertainty is evaluated by collectively varying the reconstructed four-momenta of all jets in an event, according to their η- and p_T-dependent associated uncertainties. The resulting impact on the m^*_{jjj} distributions is then assigned as the uncertainty. Moreover, to properly evaluate the systematic effect coming from differences in the JER between data and simulation, smearing is also applied to the latter by varying the jet resolutions according to their uncertainties. Both uncertainty sources are implemented as shape-altering nuisance parameters using Gaussian priors.

7.1.5 Systematic uncertainties in the signal and background rates

The uncertainties in the $PNet_W$ calibration are presented in table 2. A potential mismodeling of the W boson jet substructure dynamics, including the effects related to parton shower modeling, is corrected from the data via the SF's calibration. The corresponding SF uncertainty, 6% per jet matched to a W boson, accounts for residual jet shower mismodeling effects and the limited event sample used in the SF evaluation. In case of events with two jets matching with W bosons, the uncertainty is taken as fully correlated, e.g., for a signal event in the SRa high-p_T bin, this results in a 12% uncertainty. These are considered for both signal and background processes that contain W-boson-matched jets. The effect is accounted for by a nuisance parameter with a log-normal prior.

8 Statistical analysis and results

The search for g_{KK} resonances is performed using a binned maximum likelihood fit to the m^*_{jjj} distribution simultaneously in all ten SRs, as implemented with the CMS Combine tool [72]. The results are shown in figures 4 and 5. The lower panels show the pull distributions defined as the difference between the data and predicted event yields divided by statistical uncertainty in the data, σ_{stat}. Additionally, selected signal distributions and the total systematic uncertainty divided by σ_{stat} are displayed. The last bins include events beyond the shown range. The data are in agreement with the estimated SM background within uncertainties. The largest deviations between the data and the prediction are two single-bin downward fluctuations. These are located in SR3a and SR5b, m^*_{jjj} bin centers 3 and 2.8 TeV, with 0 and 1 data events observed for an expected 3.8 and 7.4 events, respectively. They correspond to local p-values of 2.1 and 0.5%, assuming event counts with Poisson distributions.

For the background, the leading source of systematic uncertainty lies in the estimation of the QCD multijet background rates. For the signal, the dominant uncertainty arises from the $PNet_W$ selection efficiency calibration. The overall result is statistically limited. This is presented at the lower panel of figures 4 and 5 where the ratio of systematic to statistical uncertainties $\sigma_{sys}/\sigma_{stat}$ is less than 1.

Upper limits at 95% confidence level (CL) are set on the production cross section times branching fraction for a potential resonance signal as functions of the $m_{g_{KK}}$ and m_R resonance masses, as shown in figure 6. The limits are set following the modified frequentist approach

JHEP02(2025)199

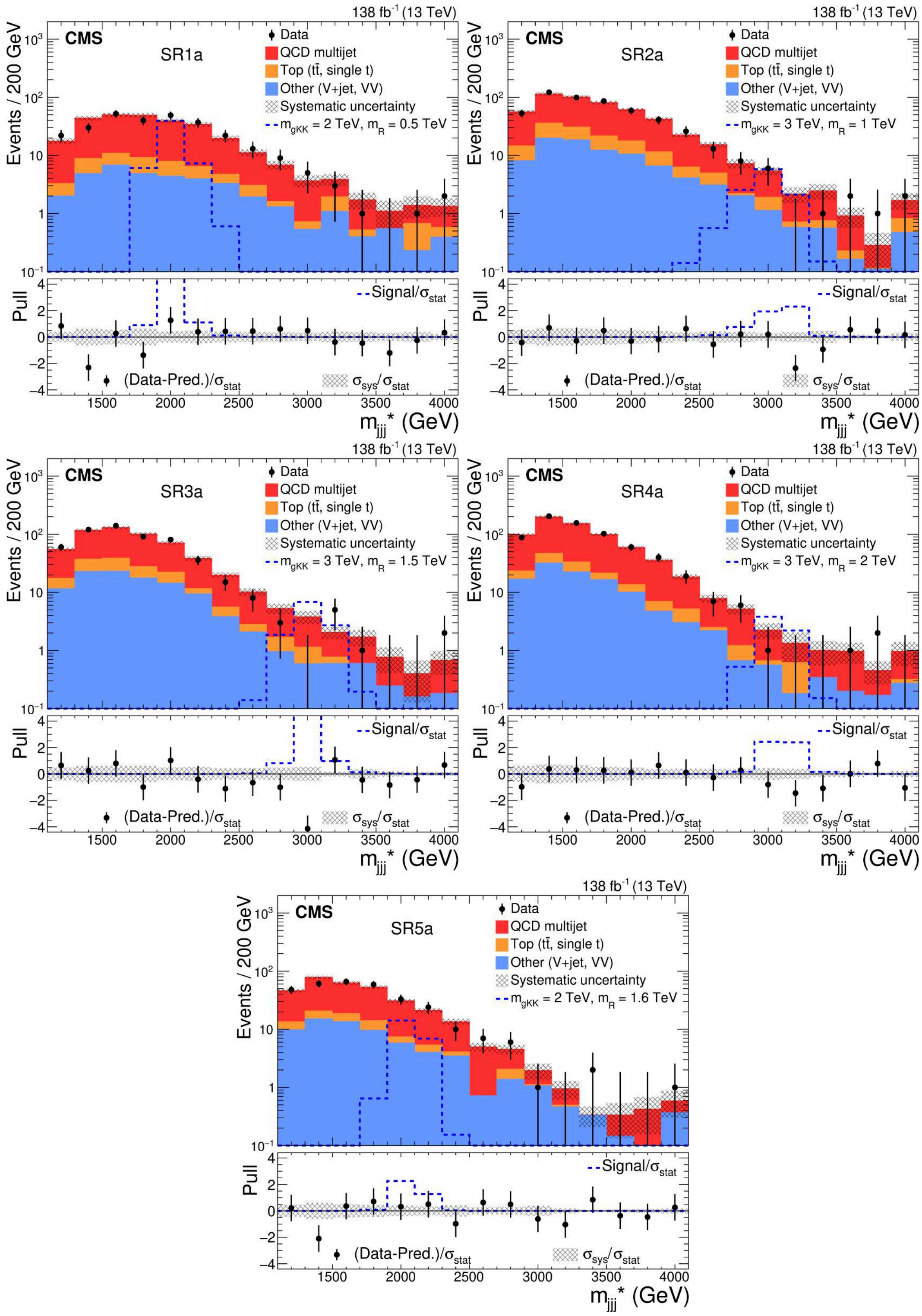

Figure 4. The m^*_{jjj} postfit spectra in the five SRxa. Upper to lower, and left to right: SR1a, SR2a, SR3a, SR4a, and SR5a. The lower panels show the pull distributions, as defined in the text, together with expected signal event yields and the systematic uncertainty normalized to σ_{stat}.

JHEP02(2025)199

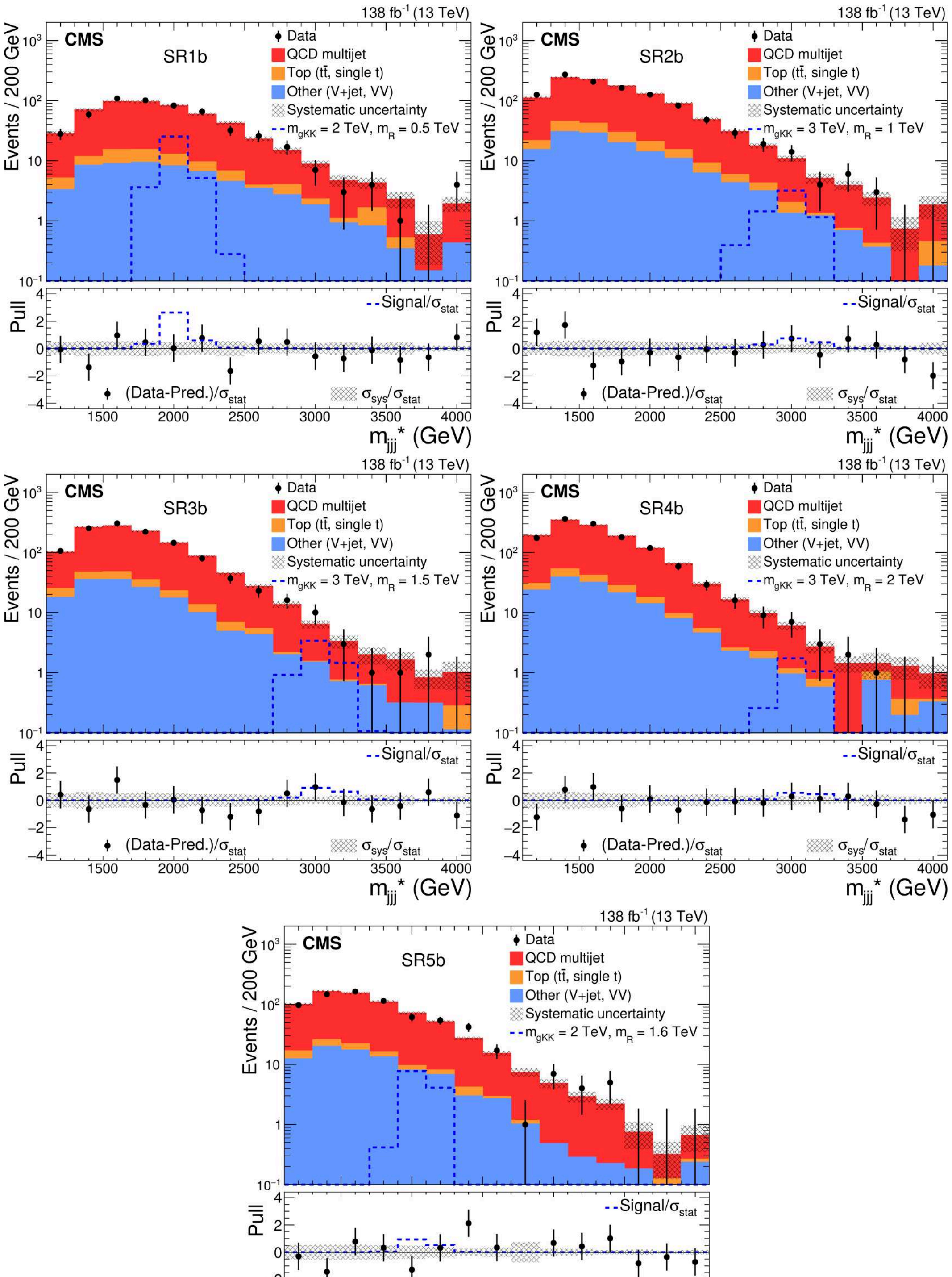

Figure 5. The $m^*_{\rm jjj}$ postfit spectra in the five SRxb. Upper to lower, and left to right: SR1b, SR2b, SR3b, SR4b, and SR5b. The lower panels show the pull distributions, as defined in the text, together with expected signal event yields and the systematic uncertainty normalized to $\sigma_{\rm stat}$.

JHEP02(2025)199

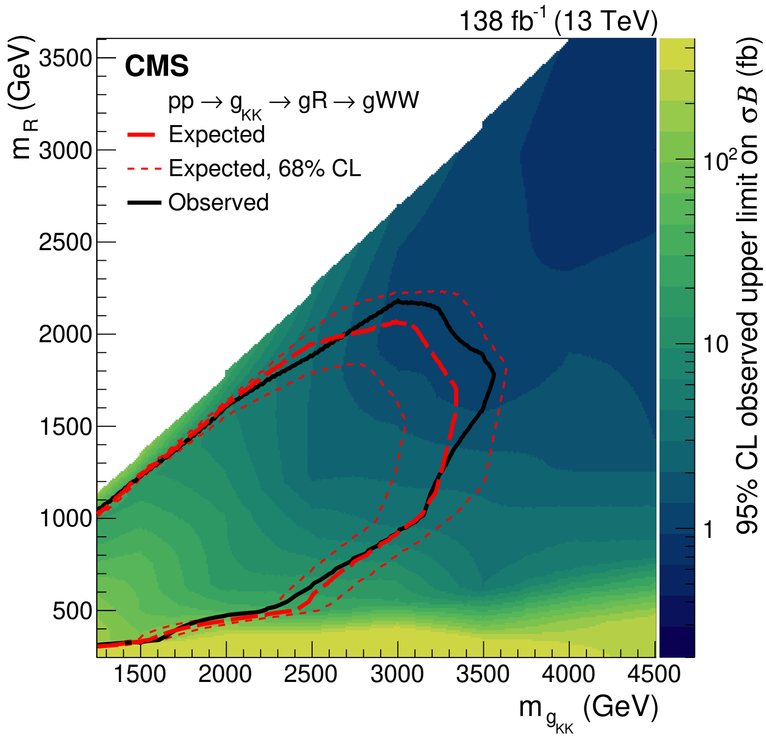

Figure 6. The 95% CL upper limits on the production cross section times branching fraction $\sigma\mathcal{B}$, for the process $pp \to g_{KK} \to gR \to gWW$. The black solid (red dashed) line contour indicates the observed (expected) exclusion region of the g_{KK} and R masses. The red dotted lines show the 68% CL band of the expected limit contour.

and the definition of the profile likelihood test statistic as described in ref. [72] using an asymptotic approximation [73].

We exclude, at 95% CL, g_{KK} resonances decaying via a scalar radion R to a gluon and two W bosons, with $m_{g_{KK}}$ in the range of 1.25–3.55 TeV and m_R in the range of 0.3–2.18 TeV, using the model provided in refs. [16–19]. The observed limits set in the $m_{g_{KK}}$–m_R plane are stronger than the expected ones because of data under-fluctuations at $m^*_{jjj} = 3.5$ TeV in SR3a and SR4a.

9 Summary

A search for heavy resonances decaying, via an intermediate resonance, to a gluon and a pair of W bosons in the all-hadronic final states has been presented. A benchmark model, in which a Kaluza-Klein gluon decays into a radion and a gluon, $g_{KK} \to gR \to gWW$, has been considered. The search is performed using proton-proton collision data at a center-of-mass energy of 13 TeV, collected by the CMS experiment, corresponding to a total integrated luminosity of 138 fb^{-1}. The final states include three large-radius jets, at least two of which are required to be massive, containing the decay products of the hadronically decaying W bosons. The topology corresponds to events where each W boson from the R decay is reconstructed as a single merged jet. In this analysis, a previously unexplored signature is probed using jet substructure techniques relying on deep learning. No resonant signal above the standard model background prediction is found in the data analyzed. Exclusion limits are set at 95% confidence level on the masses of the g_{KK} and R bosons, up to 3.55 and 2.18 TeV, respectively, and on the product of the production cross section and the branching fraction to a gluon and two W bosons in an extended warped extra-dimensional model. This result is the first analyzing the resonant WW+jet signature and complements constraints set on similar scenarios [25–28].

Acknowledgments

We congratulate our colleagues in the CERN accelerator departments for the excellent performance of the LHC and thank the technical and administrative staffs at CERN and at other CMS institutes for their contributions to the success of the CMS effort. In addition, we gratefully acknowledge the computing centers and personnel of the Worldwide LHC Computing Grid and other centers for delivering so effectively the computing infrastructure essential to our analyses. Finally, we acknowledge the enduring support for the construction and operation of the LHC, the CMS detector, and the supporting computing infrastructure provided by the following funding agencies: SC (Armenia), BMBWF and FWF (Austria); FNRS and FWO (Belgium); CNPq, CAPES, FAPERJ, FAPERGS, and FAPESP (Brazil); MES and BNSF (Bulgaria); CERN; CAS, MoST, and NSFC (China); MINCIENCIAS (Colombia); MSES and CSF (Croatia); RIF (Cyprus); SENESCYT (Ecuador); ERC PRG, RVTT3 and MoER TK202 (Estonia); Academy of Finland, MEC, and HIP (Finland); CEA and CNRS/IN2P3 (France); SRNSF (Georgia); BMBF, DFG, and HGF (Germany); GSRI (Greece); NKFIH (Hungary); DAE and DST (India); IPM (Iran); SFI (Ireland); INFN (Italy); MSIP and NRF (Republic of Korea); MES (Latvia); LMTLT (Lithuania); MOE and UM (Malaysia); BUAP, CINVESTAV, CONACYT, LNS, SEP, and UASLP-FAI (Mexico); MOS (Montenegro); MBIE (New Zealand); PAEC (Pakistan); MES and NSC (Poland); FCT (Portugal); MESTD (Serbia); MCIN/AEI and PCTI (Spain); MOSTR (Sri Lanka); Swiss Funding Agencies (Switzerland); MST (Taipei); MHESI and NSTDA (Thailand); TUBITAK and TENMAK (Turkey); NASU (Ukraine); STFC (United Kingdom); DOE and NSF (U.S.A.).

Individuals have received support from the Marie-Curie program and the European Research Council and Horizon 2020 Grant, contract Nos. 675440, 724704, 752730, 758316, 765710, 824093, 101115353, 101002207, and COST Action CA16108 (European Union); the Leventis Foundation; the Alfred P. Sloan Foundation; the Alexander von Humboldt Foundation; the Science Committee, project no. 22rl-037 (Armenia); the Belgian Federal Science Policy Office; the Fonds pour la Formation à la Recherche dans l'Industrie et dans l'Agriculture (FRIA-Belgium); the F.R.S.-FNRS and FWO (Belgium) under the "Excellence of Science — EOS" — be.h project n. 30820817; the Beijing Municipal Science & Technology Commission, No. Z191100007219010 and Fundamental Research Funds for the Central Universities (China); the Ministry of Education, Youth and Sports (MEYS) of the Czech Republic; the Shota Rustaveli National Science Foundation, grant FR-22-985 (Georgia); the Deutsche Forschungsgemeinschaft (DFG), among others, under Germany's Excellence Strategy — EXC 2121 "Quantum Universe" — 390833306, and under project number 400140256 — GRK2497; the Hellenic Foundation for Research and Innovation (HFRI), Project Number 2288 (Greece); the Hungarian Academy of Sciences, the New National

Excellence Program — ÚNKP, the NKFIH research grants K 131991, K 133046, K 138136, K 143460, K 143477, K 146913, K 146914, K 147048, 2020-2.2.1-ED-2021-00181, and TKP2021-NKTA-64 (Hungary); the Council of Science and Industrial Research, India; ICSC — National Research Center for High Performance Computing, Big Data and Quantum Computing and FAIR — Future Artificial Intelligence Research, funded by the NextGenerationEU program (Italy); the Latvian Council of Science; the Ministry of Education and Science, project no. 2022/WK/14, and the National Science Center, contracts Opus 2021/41/B/ST2/01369 and 2021/43/B/ST2/01552 (Poland); the Fundação para a Ciência e a Tecnologia, grant CEECIND/01334/2018 (Portugal); the National Priorities Research Program by Qatar National Research Fund; MCIN/AEI/10.13039/501100011033, ERDF "a way of making Europe", and the Programa Estatal de Fomento de la Investigación Científica y Técnica de Excelencia María de Maeztu, grant MDM-2017-0765 and Programa Severo Ochoa del Principado de Asturias (Spain); the Chulalongkorn Academic into Its 2nd Century Project Advancement Project, and the National Science, Research and Innovation Fund via the Program Management Unit for Human Resources & Institutional Development, Research and Innovation, grant B39G670016 (Thailand); the Kavli Foundation; the Nvidia Corporation; the SuperMicro Corporation; the Welch Foundation, contract C-1845; and the Weston Havens Foundation (U.S.A.).

Data Availability Statement. Release and preservation of data used by the CMS Collaboration as the basis for publications is guided by the CMS data preservation, re-use, and open access policy.

Code Availability Statement. The CMS core software is publicly available on GitHub.

References

[1] CMS collaboration, *Search for heavy resonances decaying to $Z(\nu\bar{\nu})V(q\bar{q}')$ in proton-proton collisions at $\sqrt{s} = 13$ TeV*, Phys. Rev. D **106** (2022) 012004 [arXiv:2109.08268] [INSPIRE].

[2] CMS collaboration, *Search for new heavy resonances decaying to WW, WZ, ZZ, WH, or ZH boson pairs in the all-jets final state in proton-proton collisions at $\sqrt{s} = 13$ TeV*, Phys. Lett. B **844** (2023) 137813 [arXiv:2210.00043] [INSPIRE].

[3] CMS collaboration, *Search for heavy resonances decaying to WW, WZ, or WH boson pairs in the lepton plus merged jet final state in proton-proton collisions at $\sqrt{s} = 13$ TeV*, Phys. Rev. D **105** (2022) 032008 [arXiv:2109.06055] [INSPIRE].

[4] CMS collaboration, *Search for high mass dijet resonances with a new background prediction method in proton-proton collisions at $\sqrt{s} = 13$ TeV*, JHEP **05** (2020) 033 [arXiv:1911.03947] [INSPIRE].

[5] CMS collaboration, *Search for a heavy resonance decaying into ZH in events with an energetic jet and two electrons, two muons, or missing transverse momentum*, CMS-PAS-B2G-23-008, CERN, Geneva, Switzerland (2024).

JHEP02(2025)199

[6] CMS collaboration, *Search for heavy resonances decaying to ZZ or ZW and axion-like particles mediating nonresonant ZZ or ZH production at* $\sqrt{s} = 13$ *TeV*, JHEP **04** (2022) 087 [arXiv:2111.13669] [INSPIRE].

[7] CMS collaboration, *Search for a heavy vector resonance decaying to a Z boson and a Higgs boson in proton-proton collisions at* $\sqrt{s} = 13$ *TeV*, Eur. Phys. J. C **81** (2021) 688 [arXiv:2102.08198] [INSPIRE].

[8] CMS collaboration, *Searches for Higgs boson production through decays of heavy resonances*, arXiv:2403.16926 [INSPIRE].

[9] ATLAS collaboration, *Search for resonances decaying into a weak vector boson and a Higgs boson in the fully hadronic final state produced in proton-proton collisions at* $\sqrt{s} = 13$ *TeV with the ATLAS detector*, Phys. Rev. D **102** (2020) 112008 [arXiv:2007.05293] [INSPIRE].

[10] ATLAS collaboration, *Search for heavy diboson resonances in semileptonic final states in pp collisions at* $\sqrt{s} = 13$ *TeV with the ATLAS detector*, Eur. Phys. J. C **80** (2020) 1165 [arXiv:2004.14636] [INSPIRE].

[11] ATLAS collaboration, *Search for diboson resonances in hadronic final states in 139 fb*$^{-1}$ *of pp collisions at* $\sqrt{s} = 13$ *TeV with the ATLAS detector*, JHEP **09** (2019) 091 [*Erratum ibid.* **06** (2020) 042] [arXiv:1906.08589] [INSPIRE].

[12] ATLAS collaboration, *Combination of searches for heavy spin-1 resonances using 139 fb*$^{-1}$ *of proton-proton collision data at* $\sqrt{s} = 13$ *TeV with the ATLAS detector*, JHEP **04** (2024) 118 [arXiv:2402.10607] [INSPIRE].

[13] ATLAS collaboration, *Search for resonant WZ production in the fully leptonic final state in proton-proton collisions at* $\sqrt{s} = 13$ *TeV with the ATLAS detector*, Eur. Phys. J. C **83** (2023) 633 [arXiv:2207.03925] [INSPIRE].

[14] ATLAS collaboration, *Search for heavy resonances decaying into a Z or W boson and a Higgs boson in final states with leptons and b-jets in 139 fb*$^{-1}$ *of pp collisions at* $\sqrt{s} = 13$ *TeV with the ATLAS detector*, JHEP **06** (2023) 016 [arXiv:2207.00230] [INSPIRE].

[15] ATLAS collaboration, *Search for new resonances in mass distributions of jet pairs using 139 fb*$^{-1}$ *of pp collisions at* $\sqrt{s} = 13$ *TeV with the ATLAS detector*, JHEP **03** (2020) 145 [arXiv:1910.08447] [INSPIRE].

[16] K. Agashe, P. Du, S. Hong and R. Sundrum, *Flavor universal resonances and warped gravity*, JHEP **01** (2017) 016 [arXiv:1608.00526] [INSPIRE].

[17] K.S. Agashe et al., *LHC signals from cascade decays of warped vector resonances*, JHEP **05** (2017) 078 [arXiv:1612.00047] [INSPIRE].

[18] K. Agashe et al., *Dedicated strategies for triboson signals from cascade decays of vector resonances*, Phys. Rev. D **99** (2019) 075016 [arXiv:1711.09920] [INSPIRE].

[19] K. Agashe et al., *Detecting a boosted diboson resonance*, JHEP **11** (2018) 027 [arXiv:1809.07334] [INSPIRE].

[20] Y.-P. Kuang, H.-Y. Ren and L.-H. Xia, *Further investigation of the model-independent probe of heavy neutral Higgs bosons at LHC run 2*, Chin. Phys. C **40** (2016) 023101 [arXiv:1506.08007] [INSPIRE].

[21] H.-Y. Ren, L.-H. Xia and Y.-P. Kuang, *Model-independent probe of anomalous heavy neutral Higgs bosons at the LHC*, Phys. Rev. D **90** (2014) 115002 [arXiv:1404.6367] [INSPIRE].

JHEP02(2025)199

[22] W.D. Goldberger and M.B. Wise, *Modulus stabilization with bulk fields*, Phys. Rev. Lett. **83** (1999) 4922 [hep-ph/9907447] [INSPIRE].

[23] S. Weinberg, *Implications of dynamical symmetry breaking*, Phys. Rev. D **13** (1976) 974 [*Erratum ibid.* **19** (1979) 1277] [INSPIRE].

[24] L. Susskind, *Dynamics of spontaneous symmetry breaking in the Weinberg-Salam theory*, Phys. Rev. D **20** (1979) 2619 [INSPIRE].

[25] CMS collaboration, *Search for resonances decaying to three W bosons in proton-proton collisions at* $\sqrt{s} = 13$ *TeV*, Phys. Rev. Lett. **129** (2022) 021802 [arXiv:2201.08476] [INSPIRE].

[26] CMS collaboration, *Search for resonances decaying to three W bosons in the hadronic final state in proton-proton collisions at* $\sqrt{s} = 13$ *TeV*, Phys. Rev. D **106** (2022) 012002 [arXiv:2112.13090] [INSPIRE].

[27] CMS collaboration, *Search for high-mass resonances decaying to a jet and a Lorentz-boosted resonance in proton-proton collisions at* $\sqrt{s} = 13$ *TeV*, Phys. Lett. B **832** (2022) 137263 [arXiv:2201.02140] [INSPIRE].

[28] CMS collaboration, *Search for narrow trijet resonances in proton-proton collisions at* $\sqrt{s} = 13$ *TeV*, Phys. Rev. Lett. **133** (2024) 011801 [arXiv:2310.14023] [INSPIRE].

[29] ATLAS collaboration, *Search for new phenomena in multi-body invariant masses in events with at least one isolated lepton and two jets using* $\sqrt{s} = 13$ *TeV proton-proton collision data collected by the ATLAS detector*, JHEP **07** (2023) 202 [arXiv:2211.08945] [INSPIRE].

[30] CMS collaboration, *Precision luminosity measurement in proton-proton collisions at* $\sqrt{s} = 13$ *TeV in 2015 and 2016 at CMS*, Eur. Phys. J. C **81** (2021) 800 [arXiv:2104.01927] [INSPIRE].

[31] CMS collaboration, *CMS luminosity measurement for the 2017 data-taking period at* $\sqrt{s} = 13$ *TeV*, CMS-PAS-LUM-17-004, CERN, Geneva, Switzerland (2018).

[32] CMS collaboration, *CMS luminosity measurement for the 2018 data-taking period at* $\sqrt{s} = 13$ *TeV*, CMS-PAS-LUM-18-002, CERN, Geneva, Switzerland (2019).

[33] CMS collaboration, *Identification of heavy, energetic, hadronically decaying particles using machine-learning techniques*, 2020 JINST **15** P06005 [arXiv:2004.08262] [INSPIRE].

[34] H. Qu and L. Gouskos, *ParticleNet: jet tagging via particle clouds*, Phys. Rev. D **101** (2020) 056019 [arXiv:1902.08570] [INSPIRE].

[35] *HEPData record for this analysis*, CMS-PAS-B2G-23-004, CERN, Geneva, Switzerland (2024).

[36] CMS collaboration, *Performance of the CMS level-1 trigger in proton-proton collisions at* $\sqrt{s} = 13$ *TeV*, 2020 JINST **15** P10017 [arXiv:2006.10165] [INSPIRE].

[37] CMS collaboration, *The CMS trigger system*, 2017 JINST **12** P01020 [arXiv:1609.02366] [INSPIRE].

[38] CMS collaboration, *The CMS experiment at the CERN LHC*, 2008 JINST **3** S08004 [INSPIRE].

[39] CMS collaboration, *Development of the CMS detector for the CERN LHC run 3*, 2024 JINST **19** P05064 [arXiv:2309.05466] [INSPIRE].

[40] J. Alwall et al., *The automated computation of tree-level and next-to-leading order differential cross sections, and their matching to parton shower simulations*, JHEP **07** (2014) 079 [arXiv:1405.0301] [INSPIRE].

JHEP02(2025)199

[41] J. Alwall et al., *Comparative study of various algorithms for the merging of parton showers and matrix elements in hadronic collisions*, *Eur. Phys. J. C* **53** (2008) 473 [arXiv:0706.2569] [INSPIRE].

[42] P. Nason, *A new method for combining NLO QCD with shower Monte Carlo algorithms*, *JHEP* **11** (2004) 040 [hep-ph/0409146] [INSPIRE].

[43] S. Frixione, P. Nason and C. Oleari, *Matching NLO QCD computations with parton shower simulations: the POWHEG method*, *JHEP* **11** (2007) 070 [arXiv:0709.2092] [INSPIRE].

[44] S. Alioli, P. Nason, C. Oleari and E. Re, *A general framework for implementing NLO calculations in shower Monte Carlo programs: the POWHEG BOX*, *JHEP* **06** (2010) 043 [arXiv:1002.2581] [INSPIRE].

[45] S. Alioli, S.-O. Moch and P. Uwer, *Hadronic top-quark pair-production with one jet and parton showering*, *JHEP* **01** (2012) 137 [arXiv:1110.5251] [INSPIRE].

[46] S. Alioli, P. Nason, C. Oleari and E. Re, *NLO single-top production matched with shower in POWHEG: s- and t-channel contributions*, *JHEP* **09** (2009) 111 [*Erratum ibid.* **02** (2010) 011] [arXiv:0907.4076] [INSPIRE].

[47] R. Frederix, E. Re and P. Torrielli, *Single-top t-channel hadroproduction in the four-flavour scheme with POWHEG and aMC@NLO*, *JHEP* **09** (2012) 130 [arXiv:1207.5391] [INSPIRE].

[48] NNPDF collaboration, *Parton distributions for the LHC run II*, *JHEP* **04** (2015) 040 [arXiv:1410.8849] [INSPIRE].

[49] T. Sjöstrand et al., *An introduction to PYTHIA 8.2*, *Comput. Phys. Commun.* **191** (2015) 159 [arXiv:1410.3012] [INSPIRE].

[50] CMS collaboration, *Extraction and validation of a new set of CMS PYTHIA8 tunes from underlying-event measurements*, *Eur. Phys. J. C* **80** (2020) 4 [arXiv:1903.12179] [INSPIRE].

[51] GEANT4 collaboration, *GEANT4 — a simulation toolkit*, *Nucl. Instrum. Meth. A* **506** (2003) 250 [INSPIRE].

[52] D. Contardo et al., *Technical proposal for the phase-II upgrade of the CMS detector*, CERN-LHCC-2015-010, CERN, Geneva, Switzerland (2015) [DOI:10.17181/CERN.VU8I.D59J].

[53] CMS collaboration, *Particle-flow reconstruction and global event description with the CMS detector*, 2017 *JINST* **12** P10003 [arXiv:1706.04965] [INSPIRE].

[54] M. Cacciari, G.P. Salam and G. Soyez, *The anti-k_t jet clustering algorithm*, *JHEP* **04** (2008) 063 [arXiv:0802.1189] [INSPIRE].

[55] M. Cacciari, G.P. Salam and G. Soyez, *FastJet user manual*, *Eur. Phys. J. C* **72** (2012) 1896 [arXiv:1111.6097] [INSPIRE].

[56] CMS collaboration, *Jet energy scale and resolution in the CMS experiment in pp collisions at 8 TeV*, 2017 *JINST* **12** P02014 [arXiv:1607.03663] [INSPIRE].

[57] CMS collaboration, *Pileup mitigation at CMS in 13 TeV data*, 2020 *JINST* **15** P09018 [arXiv:2003.00503] [INSPIRE].

[58] D. Bertolini, P. Harris, M. Low and N. Tran, *Pileup per particle identification*, *JHEP* **10** (2014) 059 [arXiv:1407.6013] [INSPIRE].

[59] CMS collaboration, *Jet algorithms performance in 13 TeV data*, CMS-PAS-JME-16-003, CERN, Geneva, Switzerland (2017).

[60] E. Bols et al., *Jet flavour classification using DeepJet*, 2020 *JINST* **15** P12012 [arXiv:2008.10519] [INSPIRE].

[61] CMS collaboration, *Performance of the DeepJet b tagging algorithm using 41.9 fb^{-1} of data from proton-proton collisions at 13 TeV with phase 1 CMS detector*, CMS-DP-2018-058, CERN, Geneva, Switzerland (2018).

[62] CMS collaboration, *Performance of missing transverse momentum reconstruction in proton-proton collisions at* $\sqrt{s} = 13$ *TeV using the CMS detector*, 2019 *JINST* **14** P07004 [arXiv:1903.06078] [INSPIRE].

[63] G. Louppe, M. Kagan and K. Cranmer, *Learning to pivot with adversarial networks*, arXiv:1611.01046 [INSPIRE].

[64] M. Dasgupta, A. Fregoso, S. Marzani and G.P. Salam, *Towards an understanding of jet substructure*, *JHEP* **09** (2013) 029 [arXiv:1307.0007] [INSPIRE].

[65] J.M. Butterworth, A.R. Davison, M. Rubin and G.P. Salam, *Jet substructure as a new Higgs search channel at the LHC*, *Phys. Rev. Lett.* **100** (2008) 242001 [arXiv:0802.2470] [INSPIRE].

[66] A.J. Larkoski, S. Marzani, G. Soyez and J. Thaler, *Soft drop*, *JHEP* **05** (2014) 146 [arXiv:1402.2657] [INSPIRE].

[67] CMS collaboration, *Identification techniques for highly boosted W bosons that decay into hadrons*, *JHEP* **12** (2014) 017 [arXiv:1410.4227] [INSPIRE].

[68] CMS collaboration, *Performance of the CMS muon detector and muon reconstruction with proton-proton collisions at* $\sqrt{s} = 13$ *TeV*, 2018 *JINST* **13** P06015 [arXiv:1804.04528] [INSPIRE].

[69] CMS collaboration, *Performance of electron reconstruction and selection with the CMS detector in proton-proton collisions at* $\sqrt{s} = 8$ *TeV*, 2015 *JINST* **10** P06005 [arXiv:1502.02701] [INSPIRE].

[70] D. Krohn, J. Thaler and L.-T. Wang, *Jet trimming*, *JHEP* **02** (2010) 084 [arXiv:0912.1342] [INSPIRE].

[71] CMS collaboration, *Measurement of the inelastic proton-proton cross section at* $\sqrt{s} = 13$ *TeV*, *JHEP* **07** (2018) 161 [arXiv:1802.02613] [INSPIRE].

[72] CMS collaboration, *The CMS statistical analysis and combination tool: combine*, *Comput. Softw. Big Sci.* **8** (2024) 19 [arXiv:2404.06614] [INSPIRE].

[73] G. Cowan, K. Cranmer, E. Gross and O. Vitells, *Asymptotic formulae for likelihood-based tests of new physics*, *Eur. Phys. J. C* **71** (2011) 1554 [*Erratum ibid.* **73** (2013) 2501] [arXiv:1007.1727] [INSPIRE].

The CMS collaboration

Yerevan Physics Institute, Yerevan, Armenia
A. Hayrapetyan, A. Tumasyan[1]

Institut für Hochenergiephysik, Vienna, Austria
W. Adam, J.W. Andrejkovic, L. Benato, T. Bergauer, S. Chatterjee, K. Damanakis, M. Dragicevic, P.S. Hussain, M. Jeitler[2], N. Krammer, A. Li, D. Liko, I. Mikulec, J. Schieck[2], R. Schöfbeck[2], D. Schwarz, M. Sonawane, W. Waltenberger, C.-E. Wulz[2]

Universiteit Antwerpen, Antwerpen, Belgium
T. Janssen, T. Van Laer, P. Van Mechelen

Vrije Universiteit Brussel, Brussel, Belgium
N. Breugelmans, J. D'Hondt, S. Dansana, A. De Moor, M. Delcourt, F. Heyen, S. Lowette, I. Makarenko, D. Müller, S. Tavernier, M. Tytgat[3], G.P. Van Onsem, S. Van Putte, D. Vannerom

Université Libre de Bruxelles, Bruxelles, Belgium
B. Bilin, B. Clerbaux, A.K. Das, I. De Bruyn, G. De Lentdecker, H. Evard, L. Favart, P. Gianneios, J. Jaramillo, A. Khalilzadeh, F.A. Khan, K. Lee, A. Malara, S. Paredes, M.A. Shahzad, L. Thomas, M. Vanden Bemden, C. Vander Velde, P. Vanlaer

Ghent University, Ghent, Belgium
M. De Coen, D. Dobur, G. Gokbulut, Y. Hong, J. Knolle, L. Lambrecht, D. Marckx, K. Mota Amarilo, K. Skovpen, N. Van Den Bossche, J. van der Linden, L. Wezenbeek

Université Catholique de Louvain, Louvain-la-Neuve, Belgium
A. Benecke, A. Bethani, G. Bruno, C. Caputo, J. De Favereau De Jeneret, C. Delaere, I.S. Donertas, A. Giammanco, A.O. Guzel, Sa. Jain, V. Lemaitre, J. Lidrych, P. Mastrapasqua, T.T. Tran

Centro Brasileiro de Pesquisas Fisicas, Rio de Janeiro, Brazil
G.A. Alves, E. Coelho, G. Correia Silva, C. Hensel, T. Menezes De Oliveira, C. Mora Herrera[4], P. Rebello Teles, M. Soeiro, A. Vilela Pereira[4]

Universidade do Estado do Rio de Janeiro, Rio de Janeiro, Brazil
W.L. Aldá Júnior, M. Barroso Ferreira Filho, H. Brandao Malbouisson, W. Carvalho, J. Chinellato[5], E.M. Da Costa, G.G. Da Silveira[6], D. De Jesus Damiao, S. Fonseca De Souza, R. Gomes De Souza, T. Laux Kuhn[6], M. Macedo, J. Martins, L. Mundim, H. Nogima, J.P. Pinheiro, A. Santoro, A. Sznajder, M. Thiel

Universidade Estadual Paulista, Universidade Federal do ABC, São Paulo, Brazil
C.A. Bernardes[6], L. Calligaris, T.R. Fernandez Perez Tomei, E.M. Gregores, I. Maietto Silverio, P.G. Mercadante, S.F. Novaes, B. Orzari, Sandra S. Padula

JHEP02(2025)199

Institute for Nuclear Research and Nuclear Energy, Bulgarian Academy of Sciences, Sofia, Bulgaria
A. Aleksandrov, G. Antchev, R. Hadjiiska, P. Iaydjiev, M. Misheva, M. Shopova, G. Sultanov

University of Sofia, Sofia, Bulgaria
A. Dimitrov, L. Litov, B. Pavlov, P. Petkov, A. Petrov, E. Shumka

Instituto De Alta Investigación, Universidad de Tarapacá, Casilla 7 D, Arica, Chile
S. Keshri, D. Laroze, S. Thakur

Beihang University, Beijing, China
T. Cheng, T. Javaid, L. Yuan

Department of Physics, Tsinghua University, Beijing, China
Z. Hu, Z. Liang, J. Liu

Institute of High Energy Physics, Beijing, China
G.M. Chen[7], H.S. Chen[7], M. Chen[7], F. Iemmi, C.H. Jiang, A. Kapoor[8], H. Liao, Z.-A. Liu[9], R. Sharma[10], J.N. Song[9], J. Tao, C. Wang[7], J. Wang, Z. Wang[7], H. Zhang, J. Zhao

State Key Laboratory of Nuclear Physics and Technology, Peking University, Beijing, China
A. Agapitos, Y. Ban, S. Deng, D. Fu, B. Guo, Q. Guo, C. Jiang, A. Levin, C. Li, Q. Li, Y. Mao, S. Qian, S.J. Qian, X. Qin, X. Sun, D. Wang, H. Yang, L. Zhang, Y. Zhao, C. Zhou

Guangdong Provincial Key Laboratory of Nuclear Science and Guangdong-Hong Kong Joint Laboratory of Quantum Matter, South China Normal University, Guangzhou, China
S. Yang

Sun Yat-Sen University, Guangzhou, China
Z. You

University of Science and Technology of China, Hefei, China
K. Jaffel, N. Lu

Nanjing Normal University, Nanjing, China
G. Bauer[11], B. Li[12], K. Yi[13], J. Zhang

Institute of Modern Physics and Key Laboratory of Nuclear Physics and Ion-beam Application (MOE) — Fudan University, Shanghai, China
Y. Li

Zhejiang University, Hangzhou, Zhejiang, China
Z. Lin, C. Lu, M. Xiao

Universidad de Los Andes, Bogota, Colombia
C. Avila, D.A. Barbosa Trujillo, A. Cabrera, C. Florez, J. Fraga, J.A. Reyes Vega

Universidad de Antioquia, Medellin, Colombia
F. Ramirez, C. Rendón, M. Rodriguez, A.A. Ruales Barbosa, J.D. Ruiz Alvarez

University of Split, Faculty of Electrical Engineering, Mechanical Engineering and Naval Architecture, Split, Croatia
D. Giljanovic, N. Godinovic, D. Lelas, A. Sculac

University of Split, Faculty of Science, Split, Croatia
M. Kovac, A. Petkovic, T. Sculac

Institute Rudjer Boskovic, Zagreb, Croatia
P. Bargassa, V. Brigljevic, B.K. Chitroda, D. Ferencek, K. Jakovcic, A. Starodumov[14], T. Susa

University of Cyprus, Nicosia, Cyprus
A. Attikis, K. Christoforou, A. Hadjiagapiou, C. Leonidou, J. Mousa, C. Nicolaou, L. Paizanos, F. Ptochos, P.A. Razis, H. Rykaczewski, H. Saka, A. Stepennov

Charles University, Prague, Czech Republic
M. Finger, M. Finger Jr., A. Kveton

Escuela Politecnica Nacional, Quito, Ecuador
E. Ayala

Universidad San Francisco de Quito, Quito, Ecuador
E. Carrera Jarrin

Academy of Scientific Research and Technology of the Arab Republic of Egypt, Egyptian Network of High Energy Physics, Cairo, Egypt
B. El-mahdy, S. Khalil[15], E. Salama[16,17]

Center for High Energy Physics (CHEP-FU), Fayoum University, El-Fayoum, Egypt
M. Abdullah Al-Mashad, M.A. Mahmoud

National Institute of Chemical Physics and Biophysics, Tallinn, Estonia
K. Ehataht, M. Kadastik, T. Lange, S. Nandan, C. Nielsen, J. Pata, M. Raidal, L. Tani, C. Veelken

Department of Physics, University of Helsinki, Helsinki, Finland
H. Kirschenmann, K. Osterberg, M. Voutilainen

JHEP02(2025)199

Helsinki Institute of Physics, Helsinki, Finland
S. Bharthuar, N. Bin Norjoharuddeen, E. Brücken, F. Garcia, P. Inkaew, K.T.S. Kallonen, T. Lampén, K. Lassila-Perini, S. Lehti, T. Lindén, M. Myllymäki, M.m. Rantanen, H. Siikonen, J. Tuominiemi

Lappeenranta-Lahti University of Technology, Lappeenranta, Finland
P. Luukka, H. Petrow

IRFU, CEA, Université Paris-Saclay, Gif-sur-Yvette, France
M. Besancon, F. Couderc, M. Dejardin, D. Denegri, J.L. Faure, F. Ferri, S. Ganjour, P. Gras, G. Hamel de Monchenault, M. Kumar, V. Lohezic, J. Malcles, F. Orlandi, L. Portales, A. Rosowsky, M.Ö. Sahin, A. Savoy-Navarro[18], P. Simkina, M. Titov, M. Tornago

Laboratoire Leprince-Ringuet, CNRS/IN2P3, Ecole Polytechnique, Institut Polytechnique de Paris, Palaiseau, France
F. Beaudette, G. Boldrini, P. Busson, A. Cappati, C. Charlot, M. Chiusi, T.D. Cuisset, F. Damas, O. Davignon, A. De Wit, I.T. Ehle, B.A. Fontana Santos Alves, S. Ghosh, A. Gilbert, R. Granier de Cassagnac, A. Hakimi, B. Harikrishnan, L. Kalipoliti, G. Liu, M. Nguyen, C. Ochando, R. Salerno, J.B. Sauvan, Y. Sirois, L. Urda Gómez, E. Vernazza, A. Zabi, A. Zghiche

Université de Strasbourg, CNRS, IPHC UMR 7178, Strasbourg, France
J.-L. Agram[19], J. Andrea, D. Apparu, D. Bloch, J.-M. Brom, E.C. Chabert, C. Collard, S. Falke, U. Goerlach, R. Haeberle, A.-C. Le Bihan, M. Meena, O. Poncet, G. Saha, M.A. Sessini, P. Van Hove, P. Vaucelle

Centre de Calcul de l'Institut National de Physique Nucleaire et de Physique des Particules, CNRS/IN2P3, Villeurbanne, France
A. Di Florio

Institut de Physique des 2 Infinis de Lyon (IP2I), Villeurbanne, France
D. Amram, S. Beauceron, B. Blancon, G. Boudoul, N. Chanon, D. Contardo, P. Depasse, C. Dozen[20], H. El Mamouni, J. Fay, S. Gascon, M. Gouzevitch, C. Greenberg, G. Grenier, B. Ille, E. Jourd'huy, I.B. Laktineh, M. Lethuillier, L. Mirabito, S. Perries, A. Purohit, M. Vander Donckt, P. Verdier, J. Xiao

Georgian Technical University, Tbilisi, Georgia
D. Chokheli, I. Lomidze, Z. Tsamalaidze[14]

RWTH Aachen University, I. Physikalisches Institut, Aachen, Germany
V. Botta, S. Consuegra Rodríguez, L. Feld, K. Klein, M. Lipinski, D. Meuser, A. Pauls, D. Pérez Adán, N. Röwert, M. Teroerde

RWTH Aachen University, III. Physikalisches Institut A, Aachen, Germany
S. Diekmann, A. Dodonova, N. Eich, D. Eliseev, F. Engelke, J. Erdmann, M. Erdmann, P. Fackeldey, B. Fischer, T. Hebbeker, K. Hoepfner, F. Ivone, A. Jung,

JHEP02(2025)199

M.y. Lee, F. Mausolf, M. Merschmeyer, A. Meyer, S. Mukherjee, D. Noll, F. Nowotny, A. Pozdnyakov, Y. Rath, W. Redjeb, F. Rehm, H. Reithler, V. Sarkisovi, A. Schmidt, C. Seth, A. Sharma, J.L. Spah, A. Stein, F. Torres Da Silva De Araujo[21], S. Wiedenbeck, S. Zaleski

RWTH Aachen University, III. Physikalisches Institut B, Aachen, Germany
C. Dziwok, G. Flügge, T. Kress, A. Nowack, O. Pooth, A. Stahl, T. Ziemons, A. Zotz

Deutsches Elektronen-Synchrotron, Hamburg, Germany
H. Aarup Petersen, M. Aldaya Martin, J. Alimena, S. Amoroso, Y. An, J. Bach, S. Baxter, M. Bayatmakou, H. Becerril Gonzalez, O. Behnke, A. Belvedere, F. Blekman[22], K. Borras[23], A. Campbell, A. Cardini, C. Cheng, F. Colombina, G. Eckerlin, D. Eckstein, L.I. Estevez Banos, E. Gallo[22], A. Geiser, V. Guglielmi, M. Guthoff, A. Hinzmann, L. Jeppe, B. Kaech, M. Kasemann, C. Kleinwort, R. Kogler, M. Komm, D. Krücker, W. Lange, D. Leyva Pernia, K. Lipka[24], W. Lohmann[25], F. Lorkowski, R. Mankel, I.-A. Melzer-Pellmann, M. Mendizabal Morentin, A.B. Meyer, G. Milella, K. Moral Figueroa, A. Mussgiller, L.P. Nair, J. Niedziela, A. Nürnberg, Y. Otarid, J. Park, E. Ranken, A. Raspereza, D. Rastorguev, J. Rübenach, L. Rygaard, A. Saggio, M. Scham[26,23], S. Schnake[23], P. Schütze, C. Schwanenberger[22], D. Selivanova, K. Sharko, M. Shchedrolosiev, D. Stafford, F. Vazzoler, A. Ventura Barroso, R. Walsh, D. Wang, Q. Wang, K. Wichmann, L. Wiens[23], C. Wissing, Y. Yang, A. Zimermmane Castro Santos

University of Hamburg, Hamburg, Germany
A. Albrecht, S. Albrecht, M. Antonello, S. Bein, S. Bollweg, M. Bonanomi, P. Connor, K. El Morabit, Y. Fischer, E. Garutti, A. Grohsjean, J. Haller, D. Hundhausen, H.R. Jabusch, G. Kasieczka, P. Keicher, R. Klanner, W. Korcari, T. Kramer, C.c. Kuo, V. Kutzner, F. Labe, J. Lange, A. Lobanov, C. Matthies, L. Moureaux, M. Mrowietz, A. Nigamova, Y. Nissan, A. Paasch, K.J. Pena Rodriguez, T. Quadfasel, B. Raciti, M. Rieger, D. Savoiu, J. Schindler, P. Schleper, M. Schröder, J. Schwandt, M. Sommerhalder, H. Stadie, G. Steinbrück, A. Tews, B. Wiederspan, M. Wolf

Karlsruher Institut fuer Technologie, Karlsruhe, Germany
S. Brommer, E. Butz, T. Chwalek, A. Dierlamm, A. Droll, U. Elicabuk, N. Faltermann, M. Giffels, A. Gottmann, F. Hartmann[27], R. Hofsaess, M. Horzela, U. Husemann, J. Kieseler, M. Klute, R. Koppenhöfer, O. Lavoryk, J.M. Lawhorn, M. Link, A. Lintuluoto, S. Maier, S. Mitra, M. Mormile, Th. Müller, M. Neukum, M. Oh, E. Pfeffer, M. Presilla, G. Quast, K. Rabbertz, B. Regnery, N. Shadskiy, I. Shvetsov, H.J. Simonis, L. Sowa, L. Stockmeier, K. Tauqeer, M. Toms, N. Trevisani, R.F. Von Cube, M. Wassmer, S. Wieland, F. Wittig, R. Wolf, X. Zuo

Institute of Nuclear and Particle Physics (INPP), NCSR Demokritos, Aghia Paraskevi, Greece
G. Anagnostou, G. Daskalakis, A. Kyriakis, A. Papadopoulos[27], A. Stakia

JHEP02(2025)199

National and Kapodistrian University of Athens, Athens, Greece
P. Kontaxakis, G. Melachroinos, Z. Painesis, I. Papavergou, I. Paraskevas, N. Saoulidou, K. Theofilatos, E. Tziaferi, K. Vellidis, I. Zisopoulos

National Technical University of Athens, Athens, Greece
G. Bakas, T. Chatzistavrou, G. Karapostoli, K. Kousouris, I. Papakrivopoulos, E. Siamarkou, G. Tsipolitis, A. Zacharopoulou

University of Ioánnina, Ioánnina, Greece
I. Bestintzanos, I. Evangelou, C. Foudas, C. Kamtsikis, P. Katsoulis, P. Kokkas, P.G. Kosmoglou Kioseoglou, N. Manthos, I. Papadopoulos, J. Strologas

HUN-REN Wigner Research Centre for Physics, Budapest, Hungary
C. Hajdu, D. Horvath[28,29], K. Márton, A.J. Rádl[30], F. Sikler, V. Veszpremi

MTA-ELTE Lendület CMS Particle and Nuclear Physics Group, Eötvös Loránd University, Budapest, Hungary
M. Csanád, K. Farkas, A. Fehérkuti[31], M.M.A. Gadallah[32], Á. Kadlecsik, P. Major, G. Pásztor, G.I. Veres

Faculty of Informatics, University of Debrecen, Debrecen, Hungary
B. Ujvari, G. Zilizi

HUN-REN ATOMKI — Institute of Nuclear Research, Debrecen, Hungary
G. Bencze, S. Czellar, J. Molnar, Z. Szillasi

Karoly Robert Campus, MATE Institute of Technology, Gyongyos, Hungary
T. Csorgo[31], F. Nemes[31], T. Novak

Panjab University, Chandigarh, India
S. Bansal, S.B. Beri, V. Bhatnagar, G. Chaudhary, S. Chauhan, N. Dhingra[33], A. Kaur, A. Kaur, H. Kaur, M. Kaur, S. Kumar, T. Sheokand, J.B. Singh, A. Singla

University of Delhi, Delhi, India
A. Ahmed, A. Bhardwaj, A. Chhetri, B.C. Choudhary, A. Kumar, A. Kumar, M. Naimuddin, K. Ranjan, M.K. Saini, S. Saumya

Saha Institute of Nuclear Physics, HBNI, Kolkata, India
S. Baradia, S. Barman[34], S. Bhattacharya, S. Das Gupta, S. Dutta, S. Dutta, S. Sarkar

Indian Institute of Technology Madras, Madras, India
M.M. Ameen, P.K. Behera, S.C. Behera, S. Chatterjee, G. Dash, P. Jana, P. Kalbhor, S. Kamble, J.R. Komaragiri[35], D. Kumar[35], T. Mishra, B. Parida[36], P.R. Pujahari, N.R. Saha, A. Sharma, A.K. Sikdar, R.K. Singh, P. Verma, S. Verma, A. Vijay

Tata Institute of Fundamental Research-A, Mumbai, India
S. Dugad, G.B. Mohanty, M. Shelake, P. Suryadevara

JHEP02(2025)199

Tata Institute of Fundamental Research-B, Mumbai, India
A. Bala, S. Banerjee, R.M. Chatterjee, M. Guchait, Sh. Jain, A. Jaiswal, S. Kumar, G. Majumder, K. Mazumdar, S. Parolia, A. Thachayath

National Institute of Science Education and Research, An OCC of Homi Bhabha National Institute, Bhubaneswar, Odisha, India
S. Bahinipati[37], C. Kar, D. Maity[38], P. Mal, V.K. Muraleedharan Nair Bindhu[38], K. Naskar[38], A. Nayak[38], S. Nayak, K. Pal, P. Sadangi, S.K. Swain, S. Varghese[38], D. Vats[38]

Indian Institute of Science Education and Research (IISER), Pune, India
S. Acharya[39], A. Alpana, S. Dube, B. Gomber[39], P. Hazarika, B. Kansal, A. Laha, B. Sahu[39], S. Sharma, K.Y. Vaish

Isfahan University of Technology, Isfahan, Iran
H. Bakhshiansohi[40], A. Jafari[41], M. Zeinali[42]

Institute for Research in Fundamental Sciences (IPM), Tehran, Iran
S. Bashiri, S. Chenarani[43], S.M. Etesami, Y. Hosseini, M. Khakzad, E. Khazaie, M. Mohammadi Najafabadi, S. Tizchang[44]

University College Dublin, Dublin, Ireland
M. Felcini, M. Grunewald

INFN Sezione di Bari[a], Università di Bari[b], Politecnico di Bari[c], Bari, Italy
M. Abbrescia[a,b], A. Colaleo[a,b], D. Creanza[a,c], B. D'Anzi[a,b], N. De Filippis[a,c], M. De Palma[a,b], W. Elmetenawee[a,b,45], N. Ferrara[a,b], L. Fiore[a], G. Iaselli[a,c], L. Longo[a], M. Louka[a,b], G. Maggi[a,c], M. Maggi[a], I. Margjeka[a], V. Mastrapasqua[a,b], S. My[a,b], S. Nuzzo[a,b], A. Pellecchia[a,b], A. Pompili[a,b], G. Pugliese[a,c], R. Radogna[a,b], D. Ramos[a], A. Ranieri[a], L. Silvestris[a], F.M. Simone[a,c], Ü. Sözbilir[a], A. Stamerra[a,b], D. Troiano[a,b], R. Venditti[a,b], P. Verwilligen[a], A. Zaza[a,b]

INFN Sezione di Bologna[a], Università di Bologna[b], Bologna, Italy
G. Abbiendi[a], C. Battilana[a,b], D. Bonacorsi[a,b], P. Capiluppi[a,b], A. Castro[†,a,b], F.R. Cavallo[a], M. Cuffiani[a,b], G.M. Dallavalle[a], T. Diotalevi[a,b], F. Fabbri[a], A. Fanfani[a,b], D. Fasanella[a], P. Giacomelli[a], L. Giommi[a,b], C. Grandi[a], L. Guiducci[a,b], S. Lo Meo[a,46], M. Lorusso[a,b], L. Lunerti[a], S. Marcellini[a], G. Masetti[a], F.L. Navarria[a,b], G. Paggi[a,b], A. Perrotta[a], F. Primavera[a,b], A.M. Rossi[a,b], S. Rossi Tisbeni[a,b], T. Rovelli[a,b], G.P. Siroli[a,b]

INFN Sezione di Catania[a], Università di Catania[b], Catania, Italy
S. Costa[a,b,47], A. Di Mattia[a], A. Lapertosa[a], R. Potenza[a,b], A. Tricomi[a,b,47], C. Tuve[a,b]

INFN Sezione di Firenze[a], Università di Firenze[b], Firenze, Italy
P. Assiouras[a], G. Barbagli[a], G. Bardelli[a,b], B. Camaiani[a,b], A. Cassese[a], R. Ceccarelli[a], V. Ciulli[a,b], C. Civinini[a], R. D'Alessandro[a,b], E. Focardi[a,b], T. Kello[a], G. Latino[a,b],

JHEP02(2025)199

P. Lenzi[a,b], M. Lizzo[a], M. Meschini[a], S. Paoletti[a], A. Papanastassiou[a,b], G. Sguazzoni[a], L. Viliani[a]

INFN Laboratori Nazionali di Frascati, Frascati, Italy

L. Benussi, S. Bianco, S. Meola[48], D. Piccolo

INFN Sezione di Genova[a], Università di Genova[b], Genova, Italy

M. Alves Gallo Pereira[a], F. Ferro[a], E. Robutti[a], S. Tosi[a,b]

INFN Sezione di Milano-Bicocca[a], Università di Milano-Bicocca[b], Milano, Italy

A. Benaglia[a], F. Brivio[a], F. Cetorelli[a,b], F. De Guio[a,b], M.E. Dinardo[a,b], P. Dini[a], S. Gennai[a], R. Gerosa[a,b], A. Ghezzi[a,b], P. Govoni[a,b], L. Guzzi[a], M.T. Lucchini[a,b], M. Malberti[a], S. Malvezzi[a], A. Massironi[a], D. Menasce[a], L. Moroni[a], M. Paganoni[a,b], S. Palluotto[a,b], D. Pedrini[a], A. Perego[a,b], B.S. Pinolini[a], G. Pizzati[a,b], S. Ragazzi[a,b], T. Tabarelli de Fatis[a,b]

INFN Sezione di Napoli[a], Università di Napoli 'Federico II'[b], Napoli, Italy; Università della Basilicata[c], Potenza, Italy; Scuola Superiore Meridionale (SSM)[d], Napoli, Italy

S. Buontempo[a], A. Cagnotta[a,b], F. Carnevali[a,b], N. Cavallo[a,c], F. Fabozzi[a,c], A.O.M. Iorio[a,b], L. Lista[a,b,49], P. Paolucci[a,27], B. Rossi[a]

INFN Sezione di Padova[a], Università di Padova[b], Padova, Italy; Università di Trento[c], Trento, Italy

R. Ardino[a], P. Azzi[a], N. Bacchetta[a,50], P. Bortignon[a], G. Bortolato[a,b], A. Bragagnolo[a,b], A.C.M. Bulla[a], R. Carlin[a,b], P. Checchia[a], T. Dorigo[a], F. Gasparini[a,b], U. Gasparini[a,b], S. Giorgetti[a], E. Lusiani[a], M. Margoni[a,b], A.T. Meneguzzo[a,b], M. Michelotto[a], M. Migliorini[a,b], F. Montecassiano[a], J. Pazzini[a,b], P. Ronchese[a,b], R. Rossin[a,b], F. Simonetto[a,b], M. Tosi[a,b], A. Triossi[a,b], S. Ventura[a], P. Zotto[a,b], A. Zucchetta[a,b], G. Zumerle[a,b]

INFN Sezione di Pavia[a], Università di Pavia[b], Pavia, Italy

A. Braghieri[a], S. Calzaferri[a], D. Fiorina[a], P. Montagna[a,b], V. Re[a], C. Riccardi[a,b], P. Salvini[a], I. Vai[a,b], P. Vitulo[a,b]

INFN Sezione di Perugia[a], Università di Perugia[b], Perugia, Italy

S. Ajmal[a,b], M.E. Ascioti[a,b], G.M. Bilei[a], C. Carrivale[a,b], D. Ciangottini[a,b], L. Fanò[a,b], M. Magherini[a,b], V. Mariani[a,b], M. Menichelli[a], F. Moscatelli[a,51], A. Rossi[a,b], A. Santocchia[a,b], D. Spiga[a], T. Tedeschi[a,b]

INFN Sezione di Pisa[a], Università di Pisa[b], Scuola Normale Superiore di Pisa[c], Pisa, Italy; Università di Siena[d], Siena, Italy

C. Aimè[a], C.A. Alexe[a,c], P. Asenov[a,b], P. Azzurri[a], G. Bagliesi[a], R. Bhattacharya[a], L. Bianchini[a,b], T. Boccali[a], E. Bossini[a], D. Bruschini[a,c], R. Castaldi[a], M.A. Ciocci[a,b], M. Cipriani[a,b], V. D'Amante[a,d], R. Dell'Orso[a], S. Donato[a], A. Giassi[a], F. Ligabue[a,c], A.C. Marini[a], D. Matos Figueiredo[a], A. Messineo[a,b], S. Mishra[a], M. Musich[a,b], F. Palla[a],

JHEP02(2025)199

A. Rizzi[a,b], G. Rolandi[a,c], S. Roy Chowdhury[a], T. Sarkar[a], A. Scribano[a], P. Spagnolo[a], R. Tenchini[a], G. Tonelli[a,b], N. Turini[a,d], F. Vaselli[a,c], A. Venturi[a], P.G. Verdini[a]

INFN Sezione di Roma[a], Sapienza Università di Roma[b], Roma, Italy

C. Baldenegro Barrera[a,b], P. Barria[a], C. Basile[a,b], F. Cavallari[a], L. Cunqueiro Mendez[a,b], D. Del Re[a,b], E. Di Marco[a,b], M. Diemoz[a], F. Errico[a,b], R. Gargiulo[a,b], E. Longo[a,b], L. Martikainen[a,b], J. Mijuskovic[a,b], G. Organtini[a,b], F. Pandolfi[a], R. Paramatti[a,b], C. Quaranta[a,b], S. Rahatlou[a,b], C. Rovelli[a], F. Santanastasio[a,b], L. Soffi[a], V. Vladimirov[a,b]

INFN Sezione di Torino[a], Università di Torino[b], Torino, Italy; Università del Piemonte Orientale[c], Novara, Italy

N. Amapane[a,b], R. Arcidiacono[a,c], S. Argiro[a,b], M. Arneodo[a,c], N. Bartosik[a], R. Bellan[a,b], A. Bellora[a,b], C. Biino[a], C. Borca[a,b], N. Cartiglia[a], M. Costa[a,b], R. Covarelli[a,b], N. Demaria[a], L. Finco[a], M. Grippo[a,b], B. Kiani[a,b], F. Legger[a], F. Luongo[a,b], C. Mariotti[a], L. Markovic[a,b], S. Maselli[a], A. Mecca[a,b], L. Menzio[a,b], P. Meridiani[a], E. Migliore[a,b], M. Monteno[a], R. Mulargia[a], M.M. Obertino[a,b], G. Ortona[a], L. Pacher[a,b], N. Pastrone[a], M. Pelliccioni[a], M. Ruspa[a,c], F. Siviero[a,b], V. Sola[a,b], A. Solano[a,b], A. Staiano[a], C. Tarricone[a,b], D. Trocino[a], G. Umoret[a,b], R. White[a,b]

INFN Sezione di Trieste[a], Università di Trieste[b], Trieste, Italy

J. Babbar[a,b], S. Belforte[a], V. Candelise[a,b], M. Casarsa[a], F. Cossutti[a], K. De Leo[a], G. Della Ricca[a,b]

Kyungpook National University, Daegu, Korea

S. Dogra, J. Hong, B. Kim, J. Kim, D. Lee, H. Lee, S.W. Lee, C.S. Moon, Y.D. Oh, M.S. Ryu, S. Sekmen, B. Tae, Y.C. Yang

Department of Mathematics and Physics — GWNU, Gangneung, Korea

M.S. Kim

Chonnam National University, Institute for Universe and Elementary Particles, Kwangju, Korea

G. Bak, P. Gwak, H. Kim, D.H. Moon

Hanyang University, Seoul, Korea

E. Asilar, J. Choi, D. Kim, T.J. Kim, J.A. Merlin, Y. Ryou

Korea University, Seoul, Korea

S. Choi, S. Han, B. Hong, K. Lee, K.S. Lee, S. Lee, J. Yoo

Kyung Hee University, Department of Physics, Seoul, Korea

J. Goh, S. Yang

Sejong University, Seoul, Korea

H. S. Kim, Y. Kim, S. Lee

JHEP02(2025)199

Seoul National University, Seoul, Korea
J. Almond, J.H. Bhyun, J. Choi, J. Choi, W. Jun, J. Kim, Y.W. Kim, S. Ko, H. Kwon, H. Lee, J. Lee, J. Lee, B.H. Oh, S.B. Oh, H. Seo, U.K. Yang, I. Yoon

University of Seoul, Seoul, Korea
W. Jang, D.Y. Kang, Y. Kang, S. Kim, B. Ko, J.S.H. Lee, Y. Lee, I.C. Park, Y. Roh, I.J. Watson

Yonsei University, Department of Physics, Seoul, Korea
S. Ha, K. Hwang, H.D. Yoo

Sungkyunkwan University, Suwon, Korea
M. Choi, M.R. Kim, H. Lee, Y. Lee, I. Yu

College of Engineering and Technology, American University of the Middle East (AUM), Dasman, Kuwait
T. Beyrouthy, Y. Gharbia

Kuwait University — College of Science — Department of Physics, Safat, Kuwait
F. Alazemi

Riga Technical University, Riga, Latvia
K. Dreimanis, A. Gaile, C. Munoz Diaz, D. Osite, G. Pikurs, A. Potrebko, M. Seidel, D. Sidiropoulos Kontos

University of Latvia (LU), Riga, Latvia
N.R. Strautnieks

Vilnius University, Vilnius, Lithuania
M. Ambrozas, A. Juodagalvis, A. Rinkevicius, G. Tamulaitis

National Centre for Particle Physics, Universiti Malaya, Kuala Lumpur, Malaysia
I. Yusuff[52], Z. Zolkapli

Universidad de Sonora (UNISON), Hermosillo, Mexico
J.F. Benitez, A. Castaneda Hernandez, H.A. Encinas Acosta, L.G. Gallegos Maríñez, M. León Coello, J.A. Murillo Quijada, A. Sehrawat, L. Valencia Palomo

Centro de Investigacion y de Estudios Avanzados del IPN, Mexico City, Mexico
G. Ayala, H. Castilla-Valdez, H. Crotte Ledesma, E. De La Cruz-Burelo, I. Heredia-De La Cruz[53], R. Lopez-Fernandez, J. Mejia Guisao, C.A. Mondragon Herrera, A. Sánchez Hernández

Universidad Iberoamericana, Mexico City, Mexico
C. Oropeza Barrera, D.L. Ramirez Guadarrama, M. Ramírez García

JHEP02(2025)199

Benemerita Universidad Autonoma de Puebla, Puebla, Mexico
I. Bautista, I. Pedraza, H.A. Salazar Ibarguen, C. Uribe Estrada

University of Montenegro, Podgorica, Montenegro
I. Bubanja, N. Raicevic

University of Canterbury, Christchurch, New Zealand
P.H. Butler

National Centre for Physics, Quaid-I-Azam University, Islamabad, Pakistan
A. Ahmad, M.I. Asghar, A. Awais, M.I.M. Awan, H.R. Hoorani, W.A. Khan

AGH University of Krakow, Krakow, Poland
V. Avati, L. Grzanka, M. Malawski

National Centre for Nuclear Research, Swierk, Poland
H. Bialkowska, M. Bluj, M. Górski, M. Kazana, M. Szleper, P. Zalewski

Institute of Experimental Physics, Faculty of Physics, University of Warsaw, Warsaw, Poland
K. Bunkowski, K. Doroba, A. Kalinowski, M. Konecki, J. Krolikowski, A. Muhammad

Warsaw University of Technology, Warsaw, Poland
P. Fokow, K. Pozniak, W. Zabolotny

Laboratório de Instrumentação e Física Experimental de Partículas, Lisboa, Portugal
M. Araujo, D. Bastos, C. Beirão Da Cruz E Silva, A. Boletti, M. Bozzo, T. Camporesi, G. Da Molin, P. Faccioli, M. Gallinaro, J. Hollar, N. Leonardo, G.B. Marozzo, A. Petrilli, M. Pisano, J. Seixas, J. Varela, J.W. Wulff

Faculty of Physics, University of Belgrade, Belgrade, Serbia
P. Adzic, P. Milenovic

VINCA Institute of Nuclear Sciences, University of Belgrade, Belgrade, Serbia
D. Devetak, M. Dordevic, J. Milosevic, L. Nadderd, V. Rekovic

Centro de Investigaciones Energéticas Medioambientales y Tecnológicas (CIEMAT), Madrid, Spain
J. Alcaraz Maestre, Cristina F. Bedoya, J.A. Brochero Cifuentes, Oliver M. Carretero, M. Cepeda, M. Cerrada, N. Colino, B. De La Cruz, A. Delgado Peris, A. Escalante Del Valle, D. Fernández Del Val, J.P. Fernández Ramos, J. Flix, M.C. Fouz, O. Gonzalez Lopez, S. Goy Lopez, J.M. Hernandez, M.I. Josa, J. Llorente Merino, C. Martin Perez, E. Martin Viscasillas, D. Moran, C. M. Morcillo Perez, Á. Navarro Tobar, C. Perez Dengra, A. Pérez-Calero Yzquierdo, J. Puerta Pelayo, I. Redondo, S. Sánchez Navas, J. Sastre, J. Vazquez Escobar

JHEP02(2025)199

Universidad Autónoma de Madrid, Madrid, Spain

J.F. de Trocóniz

Universidad de Oviedo, Instituto Universitario de Ciencias y Tecnologías Espaciales de Asturias (ICTEA), Oviedo, Spain

B. Alvarez Gonzalez, J. Cuevas, J. Fernandez Menendez, S. Folgueras, I. Gonzalez Caballero, P. Leguina, E. Palencia Cortezon, J. Prado Pico, C. Ramón Álvarez, V. Rodríguez Bouza, A. Soto Rodríguez, A. Trapote, C. Vico Villalba, P. Vischia

Instituto de Física de Cantabria (IFCA), CSIC-Universidad de Cantabria, Santander, Spain

S. Bhowmik, S. Blanco Fernández, I.J. Cabrillo, A. Calderon, J. Duarte Campderros, M. Fernandez, G. Gomez, C. Lasaosa García, R. Lopez Ruiz, C. Martinez Rivero, P. Martinez Ruiz del Arbol, F. Matorras, P. Matorras Cuevas, E. Navarrete Ramos, J. Piedra Gomez, L. Scodellaro, I. Vila, J.M. Vizan Garcia

University of Colombo, Colombo, Sri Lanka

B. Kailasapathy[54], D.D.C. Wickramarathna

University of Ruhuna, Department of Physics, Matara, Sri Lanka

W.G.D. Dharmaratna[55], K. Liyanage, N. Perera

CERN, European Organization for Nuclear Research, Geneva, Switzerland

D. Abbaneo, C. Amendola, E. Auffray, G. Auzinger, J. Baechler, D. Barney, A. Bermúdez Martínez, M. Bianco, A.A. Bin Anuar, A. Bocci, L. Borgonovi, C. Botta, E. Brondolin, C. Caillol, G. Cerminara, N. Chernyavskaya, D. d'Enterria, A. Dabrowski, A. David, A. De Roeck, M.M. Defranchis, M. Deile, M. Dobson, G. Franzoni, W. Funk, S. Giani, D. Gigi, K. Gill, F. Glege, J. Hegeman, J.K. Heikkilä, B. Huber, V. Innocente, T. James, P. Janot, O. Kaluzinska, O. Karacheban[25], S. Laurila, P. Lecoq, E. Leutgeb, C. Lourenço, L. Malgeri, M. Mannelli, M. Matthewman, A. Mehta, F. Meijers, S. Mersi, E. Meschi, V. Milosevic, F. Monti, F. Moortgat, M. Mulders, I. Neutelings, S. Orfanelli, F. Pantaleo, G. Petrucciani, A. Pfeiffer, M. Pierini, H. Qu, D. Rabady, B. Ribeiro Lopes, F. Riti, M. Rovere, H. Sakulin, R. Salvatico, S. Sanchez Cruz, S. Scarfi, C. Schwick, M. Selvaggi, A. Sharma, K. Shchelina, P. Silva, P. Sphicas[56], A.G. Stahl Leiton, A. Steen, S. Summers, D. Treille, P. Tropea, D. Walter, J. Wanczyk[57], J. Wang, K.A. Wozniak[58], S. Wuchterl, P. Zehetner, P. Zejdl, W.D. Zeuner

Paul Scherrer Institut, Villigen, Switzerland

T. Bevilacqua[59], L. Caminada[59], A. Ebrahimi, W. Erdmann, R. Horisberger, Q. Ingram, H.C. Kaestli, D. Kotlinski, C. Lange, M. Missiroli[59], L. Noehte[59], T. Rohe, A. Samalan

ETH Zurich — Institute for Particle Physics and Astrophysics (IPA), Zurich, Switzerland

T.K. Aarrestad, M. Backhaus, G. Bonomelli, A. Calandri, C. Cazzaniga, K. Datta, P. De Bryas Dexmiers D'archiac[57], A. De Cosa, G. Dissertori, M. Dittmar, M. Donegà,

F. Eble, M. Galli, K. Gedia, F. Glessgen, C. Grab, N. Härringer, T.G. Harte, D. Hits, W. Lustermann, A.-M. Lyon, R.A. Manzoni, M. Marchegiani, L. Marchese, A. Mascellani[57], F. Nessi-Tedaldi, F. Pauss, V. Perovic, S. Pigazzini, B. Ristic, R. Seidita, J. Steggemann[57], A. Tarabini, D. Valsecchi, R. Wallny

Universität Zürich, Zurich, Switzerland
C. Amsler[60], P. Bärtschi, M.F. Canelli, K. Cormier, M. Huwiler, W. Jin, A. Jofrehei, B. Kilminster, S. Leontsinis, S.P. Liechti, A. Macchiolo, P. Meiring, F. Meng, J. Motta, A. Reimers, P. Robmann, M. Senger, E. Shokr, F. Stäger, R. Tramontano

National Central University, Chung-Li, Taiwan
C. Adloff[61], D. Bhowmik, C.M. Kuo, W. Lin, P.K. Rout, P.C. Tiwari[35]

National Taiwan University (NTU), Taipei, Taiwan
L. Ceard, K.F. Chen, Z.g. Chen, A. De Iorio, W.-S. Hou, T.h. Hsu, Y.w. Kao, S. Karmakar, G. Kole, Y.y. Li, R.-S. Lu, E. Paganis, X.f. Su, J. Thomas-Wilsker, L.s. Tsai, D. Tsionou, H.y. Wu, E. Yazgan

High Energy Physics Research Unit, Department of Physics, Faculty of Science, Chulalongkorn University, Bangkok, Thailand
C. Asawatangtrakuldee, N. Srimanobhas, V. Wachirapusitanand

Çukurova University, Physics Department, Science and Art Faculty, Adana, Turkey
D. Agyel, F. Boran, F. Dolek, I. Dumanoglu[62], E. Eskut, Y. Guler[63], E. Gurpinar Guler[63], C. Isik, O. Kara, A. Kayis Topaksu, U. Kiminsu, Y. Komurcu, G. Onengut, K. Ozdemir[64], A. Polatoz, B. Tali[65], U.G. Tok, S. Turkcapar, E. Uslan, I.S. Zorbakir

Middle East Technical University, Physics Department, Ankara, Turkey
G. Sokmen, M. Yalvac[66]

Bogazici University, Istanbul, Turkey
B. Akgun, I.O. Atakisi, E. Gülmez, M. Kaya[67], O. Kaya[68], S. Tekten[69]

Istanbul Technical University, Istanbul, Turkey
A. Cakir, K. Cankocak[62,70], G.G. Dincer[62], S. Sen[71]

Istanbul University, Istanbul, Turkey
O. Aydilek[72], B. Hacisahinoglu, I. Hos[73], B. Kaynak, S. Ozkorucuklu, O. Potok, H. Sert, C. Simsek, C. Zorbilmez

Yildiz Technical University, Istanbul, Turkey
S. Cerci, B. Isildak[74], D. Sunar Cerci, T. Yetkin

Institute for Scintillation Materials of National Academy of Science of Ukraine, Kharkiv, Ukraine
A. Boyaryntsev, B. Grynyov

National Science Centre, Kharkiv Institute of Physics and Technology, Kharkiv, Ukraine
L. Levchuk

University of Bristol, Bristol, United Kingdom
D. Anthony, J.J. Brooke, A. Bundock, F. Bury, E. Clement, D. Cussans, H. Flacher, M. Glowacki, J. Goldstein, H.F. Heath, M.-L. Holmberg, L. Kreczko, S. Paramesvaran, L. Robertshaw, V.J. Smith, K. Walkingshaw Pass

Rutherford Appleton Laboratory, Didcot, United Kingdom
A.H. Ball, K.W. Bell, A. Belyaev[75], C. Brew, R.M. Brown, D.J.A. Cockerill, C. Cooke, A. Elliot, K.V. Ellis, K. Harder, S. Harper, J. Linacre, K. Manolopoulos, D.M. Newbold, E. Olaiya, D. Petyt, T. Reis, A.R. Sahasransu, G. Salvi, T. Schuh, C.H. Shepherd-Themistocleous, I.R. Tomalin, K.C. Whalen, T. Williams

Imperial College, London, United Kingdom
I. Andreou, R. Bainbridge, P. Bloch, C.E. Brown, O. Buchmuller, C.A. Carrillo Montoya, G.S. Chahal[76], D. Colling, J.S. Dancu, I. Das, P. Dauncey, G. Davies, M. Della Negra, S. Fayer, G. Fedi, G. Hall, A. Howard, G. Iles, C.R. Knight, P. Krueper, J. Langford, K.H. Law, J. León Holgado, L. Lyons, A.-M. Magnan, B. Maier, S. Mallios, M. Mieskolainen, J. Nash[77], M. Pesaresi, P.B. Pradeep, B.C. Radburn-Smith, A. Richards, A. Rose, K. Savva, C. Seez, R. Shukla, A. Tapper, K. Uchida, G.P. Uttley, T. Virdee[27], M. Vojinovic, N. Wardle, D. Winterbottom

Brunel University, Uxbridge, United Kingdom
J.E. Cole, A. Khan, P. Kyberd, I.D. Reid

Baylor University, Waco, Texas, U.S.A.
S. Abdullin, A. Brinkerhoff, E. Collins, M.R. Darwish, J. Dittmann, K. Hatakeyama, J. Hiltbrand, B. McMaster, J. Samudio, S. Sawant, C. Sutantawibul, J. Wilson

Catholic University of America, Washington, DC, U.S.A.
R. Bartek, A. Dominguez, A.E. Simsek, S.S. Yu

The University of Alabama, Tuscaloosa, Alabama, U.S.A.
B. Bam, A. Buchot Perraguin, R. Chudasama, S.I. Cooper, C. Crovella, S.V. Gleyzer, E. Pearson, C.U. Perez, P. Rumerio[78], E. Usai, R. Yi

Boston University, Boston, Massachusetts, U.S.A.
A. Akpinar, C. Cosby, G. De Castro, Z. Demiragli, C. Erice, C. Fangmeier, C. Fernandez Madrazo, E. Fontanesi, D. Gastler, F. Golf, S. Jeon, J. O‘cain, I. Reed, J. Rohlf, K. Salyer, D. Sperka, D. Spitzbart, I. Suarez, A. Tsatsos, A.G. Zecchinelli

JHEP02(2025)199

Brown University, Providence, Rhode Island, U.S.A.
G. Barone, G. Benelli, D. Cutts, L. Gouskos, M. Hadley, U. Heintz, J.M. Hogan[79], T. Kwon, G. Landsberg, K.T. Lau, J. Luo, S. Mondal, T. Russell, S. Sagir[80], X. Shen, F. Simpson, M. Stamenkovic, N. Venkatasubramanian, X. Yan

University of California, Davis, Davis, California, U.S.A.
S. Abbott, B. Barton, C. Brainerd, R. Breedon, H. Cai, M. Calderon De La Barca Sanchez, M. Chertok, M. Citron, J. Conway, P.T. Cox, R. Erbacher, F. Jensen, O. Kukral, G. Mocellin, M. Mulhearn, S. Ostrom, W. Wei, S. Yoo, F. Zhang

University of California, Los Angeles, California, U.S.A.
K. Adamidis, M. Bachtis, D. Campos, R. Cousins, A. Datta, G. Flores Avila, J. Hauser, M. Ignatenko, M.A. Iqbal, T. Lam, Y.f. Lo, E. Manca, A. Nunez Del Prado, D. Saltzberg, V. Valuev

University of California, Riverside, Riverside, California, U.S.A.
R. Clare, J.W. Gary, G. Hanson

University of California, San Diego, La Jolla, California, U.S.A.
A. Aportela, A. Arora, J.G. Branson, S. Cittolin, S. Cooperstein, D. Diaz, J. Duarte, L. Giannini, Y. Gu, J. Guiang, R. Kansal, V. Krutelyov, R. Lee, J. Letts, M. Masciovecchio, F. Mokhtar, S. Mukherjee, M. Pieri, M. Quinnan, B.V. Sathia Narayanan, V. Sharma, M. Tadel, E. Vourliotis, F. Würthwein, Y. Xiang, A. Yagil

University of California, Santa Barbara — Department of Physics, Santa Barbara, California, U.S.A.
A. Barzdukas, L. Brennan, C. Campagnari, K. Downham, C. Grieco, J. Incandela, J. Kim, A.J. Li, P. Masterson, H. Mei, J. Richman, S.N. Santpur, U. Sarica, R. Schmitz, F. Setti, J. Sheplock, D. Stuart, T.Á. Vámi, S. Wang, D. Zhang

California Institute of Technology, Pasadena, California, U.S.A.
S. Bhattacharya, A. Bornheim, O. Cerri, A. Latorre, J. Mao, H.B. Newman, G. Reales Gutiérrez, M. Spiropulu, J.R. Vlimant, C. Wang, S. Xie, R.Y. Zhu

Carnegie Mellon University, Pittsburgh, Pennsylvania, U.S.A.
J. Alison, S. An, P. Bryant, M. Cremonesi, V. Dutta, T. Ferguson, T.A. Gómez Espinosa, A. Harilal, A. Kallil Tharayil, C. Liu, T. Mudholkar, S. Murthy, P. Palit, K. Park, M. Paulini, A. Roberts, A. Sanchez, W. Terrill

University of Colorado Boulder, Boulder, Colorado, U.S.A.
J.P. Cumalat, W.T. Ford, A. Hart, A. Hassani, G. Karathanasis, N. Manganelli, J. Pearkes, C. Savard, N. Schonbeck, K. Stenson, K.A. Ulmer, S.R. Wagner, N. Zipper, D. Zuolo

JHEP02(2025)199

Cornell University, Ithaca, New York, U.S.A.
J. Alexander, S. Bright-Thonney, X. Chen, D.J. Cranshaw, J. Fan, X. Fan, S. Hogan, P. Kotamnives, J. Monroy, M. Oshiro, J.R. Patterson, M. Reid, A. Ryd, J. Thom, P. Wittich, R. Zou

Fermi National Accelerator Laboratory, Batavia, Illinois, U.S.A.
M. Albrow, M. Alyari, O. Amram, G. Apollinari, A. Apresyan, L.A.T. Bauerdick, D. Berry, J. Berryhill, P.C. Bhat, K. Burkett, J.N. Butler, A. Canepa, G.B. Cerati, H.W.K. Cheung, F. Chlebana, G. Cummings, J. Dickinson, I. Dutta, V.D. Elvira, Y. Feng, J. Freeman, A. Gandrakota, Z. Gecse, L. Gray, D. Green, A. Grummer, S. Grünendahl, D. Guerrero, O. Gutsche, R.M. Harris, R. Heller, T.C. Herwig, J. Hirschauer, B. Jayatilaka, S. Jindariani, M. Johnson, U. Joshi, T. Klijnsma, B. Klima, K.H.M. Kwok, S. Lammel, C. Lee, D. Lincoln, R. Lipton, T. Liu, C. Madrid, K. Maeshima, C. Mantilla, D. Mason, P. McBride, P. Merkel, S. Mrenna, S. Nahn, J. Ngadiuba, D. Noonan, S. Norberg, V. Papadimitriou, N. Pastika, K. Pedro, C. Pena[81], F. Ravera, A. Reinsvold Hall[82], L. Ristori, M. Safdari, E. Sexton-Kennedy, N. Smith, A. Soha, L. Spiegel, S. Stoynev, J. Strait, L. Taylor, S. Tkaczyk, N.V. Tran, L. Uplegger, E.W. Vaandering, I. Zoi

University of Florida, Gainesville, Florida, U.S.A.
C. Aruta, P. Avery, D. Bourilkov, P. Chang, V. Cherepanov, R.D. Field, C. Huh, E. Koenig, M. Kolosova, J. Konigsberg, A. Korytov, K. Matchev, N. Menendez, G. Mitselmakher, K. Mohrman, A. Muthirakalayil Madhu, N. Rawal, S. Rosenzweig, Y. Takahashi, J. Wang

Florida State University, Tallahassee, Florida, U.S.A.
T. Adams, A. Al Kadhim, A. Askew, S. Bower, R. Hashmi, R.S. Kim, S. Kim, T. Kolberg, G. Martinez, H. Prosper, P.R. Prova, M. Wulansatiti, R. Yohay, J. Zhang

Florida Institute of Technology, Melbourne, Florida, U.S.A.
B. Alsufyani, M.M. Baarmand, S. Butalla, S. Das, T. Elkafrawy[17], M. Hohlmann, E. Yanes

University of Illinois Chicago, Chicago, Illinois, U.S.A.
M.R. Adams, A. Baty, C. Bennett, R. Cavanaugh, R. Escobar Franco, O. Evdokimov, C.E. Gerber, M. Hawksworth, A. Hingrajiya, D.J. Hofman, J.h. Lee, D. S. Lemos, A.H. Merrit, C. Mills, S. Nanda, G. Oh, B. Ozek, D. Pilipovic, R. Pradhan, E. Prifti, T. Roy, S. Rudrabhatla, N. Singh, M.B. Tonjes, N. Varelas, M.A. Wadud, Z. Ye, J. Yoo

The University of Iowa, Iowa City, Iowa, U.S.A.
M. Alhusseini, D. Blend, K. Dilsiz[83], L. Emediato, G. Karaman, O.K. Köseyan, J.-P. Merlo, A. Mestvirishvili[84], O. Neogi, H. Ogul[85], Y. Onel, A. Penzo, C. Snyder, E. Tiras[86]

JHEP02(2025)199

Johns Hopkins University, Baltimore, Maryland, U.S.A.
B. Blumenfeld, L. Corcodilos, J. Davis, A.V. Gritsan, L. Kang, S. Kyriacou, P. Maksimovic, M. Roguljic, J. Roskes, S. Sekhar, M. Swartz

The University of Kansas, Lawrence, Kansas, U.S.A.
A. Abreu, L.F. Alcerro Alcerro, J. Anguiano, S. Arteaga Escatel, P. Baringer, A. Bean, Z. Flowers, D. Grove, J. King, G. Krintiras, M. Lazarovits, C. Le Mahieu, J. Marquez, M. Murray, M. Nickel, M. Pitt, S. Popescu[87], C. Rogan, C. Royon, S. Sanders, C. Smith, G. Wilson

Kansas State University, Manhattan, Kansas, U.S.A.
B. Allmond, R. Gujju Gurunadha, A. Ivanov, K. Kaadze, Y. Maravin, J. Natoli, D. Roy, G. Sorrentino

University of Maryland, College Park, Maryland, U.S.A.
A. Baden, A. Belloni, J. Bistany-riebman, Y.M. Chen, S.C. Eno, N.J. Hadley, S. Jabeen, R.G. Kellogg, T. Koeth, B. Kronheim, Y. Lai, S. Lascio, A.C. Mignerey, S. Nabili, C. Palmer, C. Papageorgakis, M.M. Paranjpe, E. Popova[88], A. Shevelev, L. Wang

Massachusetts Institute of Technology, Cambridge, Massachusetts, U.S.A.
J. Bendavid, I.A. Cali, P.c. Chou, M. D'Alfonso, J. Eysermans, C. Freer, G. Gomez-Ceballos, M. Goncharov, G. Grosso, P. Harris, D. Hoang, D. Kovalskyi, J. Krupa, L. Lavezzo, Y.-J. Lee, K. Long, C. Mcginn, A. Novak, M.I. Park, C. Paus, C. Reissel, C. Roland, G. Roland, S. Rothman, G.S.F. Stephans, Z. Wang, B. Wyslouch, T. J. Yang

University of Minnesota, Minneapolis, Minnesota, U.S.A.
B. Crossman, B.M. Joshi, C. Kapsiak, M. Krohn, D. Mahon, J. Mans, B. Marzocchi, M. Revering, R. Rusack, R. Saradhy, N. Strobbe

University of Nebraska-Lincoln, Lincoln, Nebraska, U.S.A.
K. Bloom, D.R. Claes, G. Haza, J. Hossain, C. Joo, I. Kravchenko, J.E. Siado, W. Tabb, A. Vagnerini, A. Wightman, F. Yan, D. Yu

State University of New York at Buffalo, Buffalo, New York, U.S.A.
H. Bandyopadhyay, L. Hay, H.w. Hsia, I. Iashvili, A. Kalogeropoulos, A. Kharchilava, M. Morris, D. Nguyen, S. Rappoccio, H. Rejeb Sfar, A. Williams, P. Young

Northeastern University, Boston, Massachusetts, U.S.A.
G. Alverson, E. Barberis, J. Bonilla, B. Bylsma, M. Campana, J. Dervan, Y. Haddad, Y. Han, I. Israr, A. Krishna, J. Li, M. Lu, G. Madigan, R. Mccarthy, D.M. Morse, V. Nguyen, T. Orimoto, A. Parker, L. Skinnari, D. Wood

Northwestern University, Evanston, Illinois, U.S.A.
J. Bueghly, S. Dittmer, K.A. Hahn, D. Li, Y. Liu, M. Mcginnis, Y. Miao, D.G. Monk, M.H. Schmitt, A. Taliercio, M. Velasco

University of Notre Dame, Notre Dame, Indiana, U.S.A.
G. Agarwal, R. Band, R. Bucci, S. Castells, A. Das, R. Goldouzian, M. Hildreth, K.W. Ho, K. Hurtado Anampa, T. Ivanov, C. Jessop, K. Lannon, J. Lawrence, N. Loukas, L. Lutton, J. Mariano, N. Marinelli, I. Mcalister, T. McCauley, C. Mcgrady, C. Moore, Y. Musienko[14], H. Nelson, M. Osherson, A. Piccinelli, R. Ruchti, A. Townsend, Y. Wan, M. Wayne, H. Yockey, M. Zarucki, L. Zygala

The Ohio State University, Columbus, Ohio, U.S.A.
A. Basnet, M. Carrigan, L.S. Durkin, C. Hill, M. Joyce, M. Nunez Ornelas, K. Wei, D.A. Wenzl, B.L. Winer, B. R. Yates

Princeton University, Princeton, New Jersey, U.S.A.
H. Bouchamaoui, K. Coldham, P. Das, G. Dezoort, P. Elmer, A. Frankenthal, B. Greenberg, N. Haubrich, K. Kennedy, G. Kopp, S. Kwan, D. Lange, A. Loeliger, D. Marlow, I. Ojalvo, J. Olsen, D. Stickland, C. Tully, L.H. Vage

University of Puerto Rico, Mayaguez, Puerto Rico, U.S.A.
S. Malik, R. Sharma

Purdue University, West Lafayette, Indiana, U.S.A.
A.S. Bakshi, S. Chandra, R. Chawla, A. Gu, L. Gutay, M. Jones, A.W. Jung, A.M. Koshy, M. Liu, G. Negro, N. Neumeister, G. Paspalaki, S. Piperov, V. Scheurer, J.F. Schulte, M. Stojanovic, J. Thieman, A. K. Virdi, F. Wang, A. Wildridge, W. Xie, Y. Yao

Purdue University Northwest, Hammond, Indiana, U.S.A.
J. Dolen, N. Parashar, A. Pathak

Rice University, Houston, Texas, U.S.A.
D. Acosta, T. Carnahan, K.M. Ecklund, P.J. Fernández Manteca, S. Freed, P. Gardner, F.J.M. Geurts, I. Krommydas, W. Li, J. Lin, O. Miguel Colin, B.P. Padley, R. Redjimi, J. Rotter, E. Yigitbasi, Y. Zhang

University of Rochester, Rochester, New York, U.S.A.
A. Bodek, P. de Barbaro, R. Demina, J.L. Dulemba, A. Garcia-Bellido, O. Hindrichs, A. Khukhunaishvili, N. Parmar, P. Parygin[88], R. Taus

Rutgers, The State University of New Jersey, Piscataway, New Jersey, U.S.A.
B. Chiarito, J.P. Chou, S.V. Clark, D. Gadkari, Y. Gershtein, E. Halkiadakis, M. Heindl, C. Houghton, D. Jaroslawski, S. Konstantinou, I. Laflotte, A. Lath, R. Montalvo, K. Nash, J. Reichert, H. Routray, P. Saha, S. Salur, S. Schnetzer, S. Somalwar, R. Stone, S.A. Thayil, S. Thomas, J. Vora, H. Wang

University of Tennessee, Knoxville, Tennessee, U.S.A.
D. Ally, A.G. Delannoy, S. Fiorendi, S. Higginbotham, T. Holmes, A.R. Kanuganti, N. Karunarathna, L. Lee, E. Nibigira, S. Spanier

Texas A&M University, College Station, Texas, U.S.A.
D. Aebi, M. Ahmad, T. Akhter, K. Androsov[57], O. Bouhali[89], R. Eusebi, J. Gilmore, T. Huang, T. Kamon[90], H. Kim, S. Luo, R. Mueller, D. Overton, D. Rathjens, A. Safonov

Texas Tech University, Lubbock, Texas, U.S.A.
N. Akchurin, J. Damgov, N. Gogate, V. Hegde, A. Hussain, Y. Kazhykarim, K. Lamichhane, S.W. Lee, A. Mankel, T. Peltola, I. Volobouev

Vanderbilt University, Nashville, Tennessee, U.S.A.
E. Appelt, Y. Chen, S. Greene, A. Gurrola, W. Johns, R. Kunnawalkam Elayavalli, A. Melo, F. Romeo, P. Sheldon, S. Tuo, J. Velkovska, J. Viinikainen

University of Virginia, Charlottesville, Virginia, U.S.A.
B. Cardwell, H. Chung, B. Cox, J. Hakala, R. Hirosky, A. Ledovskoy, C. Neu

Wayne State University, Detroit, Michigan, U.S.A.
S. Bhattacharya, P.E. Karchin

University of Wisconsin — Madison, Madison, Wisconsin, U.S.A.
A. Aravind, S. Banerjee, K. Black, T. Bose, E. Chavez, S. Dasu, P. Everaerts, C. Galloni, H. He, M. Herndon, A. Herve, C.K. Koraka, A. Lanaro, R. Loveless, J. Madhusudanan Sreekala, A. Mallampalli, A. Mohammadi, S. Mondal, G. Parida, L. Pétré, D. Pinna, A. Savin, V. Shang, V. Sharma, W.H. Smith, D. Teague, H.F. Tsoi, W. Vetens, A. Warden

Authors affiliated with an institute or an international laboratory covered by a cooperation agreement with CERN
S. Afanasiev, V. Alexakhin, D. Budkouski, I. Golutvin[†], I. Gorbunov, V. Karjavine, V. Korenkov, A. Lanev, A. Malakhov, V. Matveev[91], V. Palichik, V. Perelygin, M. Savina, V. Shalaev, S. Shmatov, S. Shulha, V. Smirnov, O. Teryaev, N. Voytishin, B.S. Yuldashev[92], A. Zarubin, I. Zhizhin, G. Gavrilov, V. Golovtcov, Y. Ivanov, V. Kim[91], P. Levchenko[93], V. Murzin, V. Oreshkin, D. Sosnov, V. Sulimov, L. Uvarov, A. Vorobyev[†], Yu. Andreev, A. Dermenev, S. Gninenko, N. Golubev, A. Karneyeu, D. Kirpichnikov, M. Kirsanov, N. Krasnikov, I. Tlisova, A. Toropin, T. Aushev, K. Ivanov, V. Gavrilov, N. Lychkovskaya, A. Nikitenko[94,95], V. Popov, A. Zhokin, M. Chadeeva[91], R. Chistov[91], S. Polikarpov[91], V. Andreev, M. Azarkin, M. Kirakosyan, A. Terkulov, E. Boos, V. Bunichev, M. Dubinin[81], L. Dudko, A. Ershov, A. Gribushin, V. Klyukhin, O. Kodolova[95], S. Obraztsov, S. Petrushanko, V. Savrin, A. Snigirev, V. Blinov[91], T. Dimova[91], A. Kozyrev[91], O. Radchenko[91], Y. Skovpen[91], V. Kachanov, D. Konstantinov, S. Slabospitskii, A. Uzunian, A. Babaev, V. Borshch, D. Druzhkin[96]

[†] *Deceased*
[1] *Also at Yerevan State University, Yerevan, Armenia*
[2] *Also at TU Wien, Vienna, Austria*
[3] *Also at Ghent University, Ghent, Belgium*

JHEP02(2025)199

[4] *Also at Universidade do Estado do Rio de Janeiro, Rio de Janeiro, Brazil*
[5] *Also at Universidade Estadual de Campinas, Campinas, Brazil*
[6] *Also at Federal University of Rio Grande do Sul, Porto Alegre, Brazil*
[7] *Also at University of Chinese Academy of Sciences, Beijing, China*
[8] *Also at China Center of Advanced Science and Technology, Beijing, China*
[9] *Also at University of Chinese Academy of Sciences, Beijing, China*
[10] *Also at China Spallation Neutron Source, Guangdong, China*
[11] *Now at Henan Normal University, Xinxiang, China*
[12] *Also at University of Shanghai for Science and Technology, Shanghai, China*
[13] *Now at The University of Iowa, Iowa City, Iowa, U.S.A.*
[14] *Also at an institute or an international laboratory covered by a cooperation agreement with CERN*
[15] *Also at Zewail City of Science and Technology, Zewail, Egypt*
[16] *Also at British University in Egypt, Cairo, Egypt*
[17] *Now at Ain Shams University, Cairo, Egypt*
[18] *Also at Purdue University, West Lafayette, Indiana, U.S.A.*
[19] *Also at Université de Haute Alsace, Mulhouse, France*
[20] *Also at Istinye University, Istanbul, Turkey*
[21] *Also at The University of the State of Amazonas, Manaus, Brazil*
[22] *Also at University of Hamburg, Hamburg, Germany*
[23] *Also at RWTH Aachen University, III. Physikalisches Institut A, Aachen, Germany*
[24] *Also at Bergische University Wuppertal (BUW), Wuppertal, Germany*
[25] *Also at Brandenburg University of Technology, Cottbus, Germany*
[26] *Also at Forschungszentrum Jülich, Juelich, Germany*
[27] *Also at CERN, European Organization for Nuclear Research, Geneva, Switzerland*
[28] *Also at HUN-REN ATOMKI — Institute of Nuclear Research, Debrecen, Hungary*
[29] *Now at Universitatea Babes-Bolyai — Facultatea de Fizica, Cluj-Napoca, Romania*
[30] *Also at MTA-ELTE Lendület CMS Particle and Nuclear Physics Group, Eötvös Loránd University, Budapest, Hungary*
[31] *Also at HUN-REN Wigner Research Centre for Physics, Budapest, Hungary*
[32] *Also at Physics Department, Faculty of Science, Assiut University, Assiut, Egypt*
[33] *Also at Punjab Agricultural University, Ludhiana, India*
[34] *Also at University of Visva-Bharati, Santiniketan, India*
[35] *Also at Indian Institute of Science (IISc), Bangalore, India*
[36] *Also at Amity University Uttar Pradesh, Noida, India*
[37] *Also at IIT Bhubaneswar, Bhubaneswar, India*
[38] *Also at Institute of Physics, Bhubaneswar, India*
[39] *Also at University of Hyderabad, Hyderabad, India*
[40] *Also at Deutsches Elektronen-Synchrotron, Hamburg, Germany*
[41] *Also at Isfahan University of Technology, Isfahan, Iran*
[42] *Also at Sharif University of Technology, Tehran, Iran*
[43] *Also at Department of Physics, University of Science and Technology of Mazandaran, Behshahr, Iran*
[44] *Also at Department of Physics, Faculty of Science, Arak University, ARAK, Iran*
[45] *Also at Helwan University, Cairo, Egypt*
[46] *Also at Italian National Agency for New Technologies, Energy and Sustainable Economic Development, Bologna, Italy*
[47] *Also at Centro Siciliano di Fisica Nucleare e di Struttura Della Materia, Catania, Italy*
[48] *Also at Università degli Studi Guglielmo Marconi, Roma, Italy*
[49] *Also at Scuola Superiore Meridionale, Università di Napoli 'Federico II', Napoli, Italy*
[50] *Also at Fermi National Accelerator Laboratory, Batavia, Illinois, U.S.A.*
[51] *Also at Consiglio Nazionale delle Ricerche — Istituto Officina dei Materiali, Perugia, Italy*
[52] *Also at Department of Applied Physics, Faculty of Science and Technology, Universiti Kebangsaan Malaysia, Bangi, Malaysia*
[53] *Also at Consejo Nacional de Ciencia y Tecnología, Mexico City, Mexico*

JHEP02(2025)199

[54] Also at Trincomalee Campus, Eastern University, Sri Lanka, Nilaveli, Sri Lanka
[55] Also at Saegis Campus, Nugegoda, Sri Lanka
[56] Also at National and Kapodistrian University of Athens, Athens, Greece
[57] Also at Ecole Polytechnique Fédérale Lausanne, Lausanne, Switzerland
[58] Also at University of Vienna, Vienna, Austria
[59] Also at Universität Zürich, Zurich, Switzerland
[60] Also at Stefan Meyer Institute for Subatomic Physics, Vienna, Austria
[61] Also at Laboratoire d'Annecy-le-Vieux de Physique des Particules, IN2P3-CNRS, Annecy-le-Vieux, France
[62] Also at Near East University, Research Center of Experimental Health Science, Mersin, Turkey
[63] Also at Konya Technical University, Konya, Turkey
[64] Also at Izmir Bakircay University, Izmir, Turkey
[65] Also at Adiyaman University, Adiyaman, Turkey
[66] Also at Bozok Universitetesi Rektörlügü, Yozgat, Turkey
[67] Also at Marmara University, Istanbul, Turkey
[68] Also at Milli Savunma University, Istanbul, Turkey
[69] Also at Kafkas University, Kars, Turkey
[70] Now at Istanbul Okan University, Istanbul, Turkey
[71] Also at Hacettepe University, Ankara, Turkey
[72] Also at Erzincan Binali Yildirim University, Erzincan, Turkey
[73] Also at Istanbul University — Cerrahpasa, Faculty of Engineering, Istanbul, Turkey
[74] Also at Yildiz Technical University, Istanbul, Turkey
[75] Also at School of Physics and Astronomy, University of Southampton, Southampton, United Kingdom
[76] Also at IPPP Durham University, Durham, United Kingdom
[77] Also at Monash University, Faculty of Science, Clayton, Australia
[78] Also at Università di Torino, Torino, Italy
[79] Also at Bethel University, St. Paul, Minnesota, U.S.A.
[80] Also at Karamanoğlu Mehmetbey University, Karaman, Turkey
[81] Also at California Institute of Technology, Pasadena, California, U.S.A.
[82] Also at United States Naval Academy, Annapolis, Maryland, U.S.A.
[83] Also at Bingol University, Bingol, Turkey
[84] Also at Georgian Technical University, Tbilisi, Georgia
[85] Also at Sinop University, Sinop, Turkey
[86] Also at Erciyes University, Kayseri, Turkey
[87] Also at Horia Hulubei National Institute of Physics and Nuclear Engineering (IFIN-HH), Bucharest, Romania
[88] Now at another institute or international laboratory covered by a cooperation agreement with CERN
[89] Also at Texas A&M University at Qatar, Doha, Qatar
[90] Also at Kyungpook National University, Daegu, Korea
[91] Also at another institute or international laboratory covered by a cooperation agreement with CERN
[92] Also at Institute of Nuclear Physics of the Uzbekistan Academy of Sciences, Tashkent, Uzbekistan
[93] Also at Northeastern University, Boston, Massachusetts, U.S.A.
[94] Also at Imperial College, London, United Kingdom
[95] Now at Yerevan Physics Institute, Yerevan, Armenia
[96] Also at Universiteit Antwerpen, Antwerpen, Belgium

JHEP02(2025)199